JEM Journal of Experimental Medicine

ARTICLE

B-1 plasma cells require non-cognate CD4 T cell help to generate a unique repertoire of natural IgM

Fauna L. Smith[1,2], Hannah P. Savage[1,3], Zheng Luo[1], Christopher M. Tipton[5,7], F. Eun-Hyung Lee[6,7], April C. Apostol[4], Anna E. Beaudin[4], Diego A. Lopez[4], Ingvill Jensen[1], Stefan Keller[8], and Nicole Baumgarth[1,2,3,8]

Evolutionarily conserved, "natural" (n)IgM is broadly reactive to both self and foreign antigens. Its selective deficiency leads to increases in autoimmune diseases and infections. In mice, nIgM is secreted independent of microbial exposure to bone marrow (BM) and spleen B-1 cell–derived plasma cells (B-1PC), generating the majority of nIgM, or by B-1 cells that remain non-terminally differentiated (B-1_{sec}). Thus, it has been assumed that the nIgM repertoire is broadly reflective of the repertoire of body cavity B-1 cells. Studies here reveal, however, that B-1PC generate a distinct, oligoclonal nIgM repertoire, characterized by short CDR3 variable immunoglobulin heavy chain regions, 7–8 amino acids in length, some public, many arising from convergent rearrangements, while specificities previously associated with nIgM were generated by a population of IgM-secreting B-1 (B-1_{sec}). BM, but not spleen B-1PC, or B-1_{sec} also required the presence of TCRαβ CD4 T cells for their development from fetal precursors. Together, the studies identify important previously unknown characteristics of the nIgM pool.

Introduction

Natural IgM (nIgM) are spontaneously generated, self-reactive, circulating antibodies that can be produced independent of foreign antigen exposure and apparently independent of T cells (Hooijkaas et al., 1985; Van Oudenaren et al., 1984; Madsen et al., 1999) by antibody-secreting cells (ASC) located primarily in the bone marrow (BM) and spleen (Hayakawa et al., 1984; Savage et al., 2017; Choi et al., 2012; Förster and Rajewsky, 1987; Kawahara et al., 2003). Selective IgM deficiency, a rare human condition, leads to increased rates of infections and autoimmune disease. 30–45% of human patients with selective IgM deficiency have higher incidences of asthma and allergic rhinitis (Goldstein et al., 2006), as well as systemic lupus erythematosus and Hashimoto's thyroiditis compared with the general population (Takeuchi et al., 2009; Gupta and Gupta, 2017). Also, humans with selective IgM deficiency are more likely to suffer from chronic and opportunistic infections (Gupta and Gupta, 2017).

Mice with defects in secreted IgM show similar disease phenotypes to those observed in humans. They develop autoimmune diseases and have elevated levels of anti-nuclear, anti-single, and anti-double stranded DNA antibodies (Boes et al., 2000; Ehrenstein et al., 2000; Notley et al., 2011; Nguyen et al., 2015). Mechanisms remain to be more fully explored but might involve reduced IgM-mediated opsonization and uptake of autoantigens (Ogden et al., 2009; Quartier et al., 2005; Chen et al., 2009), a failure to block the biological effects of oxidized phospholipids leading to chronic inflammation (Que et al., 2018) and/or alterations in central tolerance induction (Nguyen et al., 2015). nIgM also protects against replication and dissemination of many bacterial, fungal, and viral pathogens (Baumgarth et al., 2000; Haas et al., 2005; Wardemann et al., 2002; Ochsenbein et al., 1999; Smith and Baumgarth, 2019; Zeng et al., 2018; Jackson-Jones et al., 2016; Alugupalli and Gerstein, 2005). It can do so by directly neutralizing pathogens, such as *Streptococcus pneumoniae*, influenza virus, and *Borrelia hermsii* (Alugupalli et al., 2003; Jayasekera et al., 2007; Ehrenstein and Notley, 2010) and by supporting

[1]Center for Immunology and Infectious Diseases, University of California, Davis, Davis, CA, USA; [2]Integrated Pathobiology Graduate Group, University of California, Davis, Davis, CA, USA; [3]Graduate Group in Immunology, University of California, Davis, Davis, CA, USA; [4]Division of Hematology and Hematologic Malignancies, University of Utah, Salt Lake City, UT, USA; [5]Department of Medicine, Division of Rheumatology, Emory University, Atlanta, GA, USA; [6]Department of Medicine, Division of Pulmonary, Allergy, Critical Care, and Sleep Medicine, Emory University, Atlanta, GA, USA; [7]Lowance Center for Human Immunology, Emory University, Atlanta, GA, USA; [8]Department Pathology, Microbiology & Immunology, School of Veterinary Medicine, University of California, Davis, Davis, CA, USA.

Correspondence to Nicole Baumgarth: nbaumga3@jhmi.edu

H.P. Savage's current affiliation is Department Medical Microbiology & Immunology School of Medicine University of California, Davis, Davis, CA, USA. I. Jensen's current affiliation is Norwegian College of Fishery Science Faculty of Biosciences, Fisheries and Economics UiT The Arctic University of Norway, Tromsø, Norway.

the induction of maximal antigen-specific IgG responses by conventional B-2 cells (Baumgarth et al., 2000; Yuan et al., 2012; Boes et al., 1998; Nguyen et al., 2017; Heyman, 2000). The lack of nIgM was also shown to attenuate adaptive T cell responses to neoantigens during cancer development (Atif et al., 2018).

Although serum nIgM levels and frequencies of IgM-ASC in BM and spleen are comparable between mice held under germ-free/antigen-free conditions and those housed under specific pathogen–free (SPF) conditions (Savage et al., 2017; Bos et al., 1989; Haury et al., 1997), the nIgM repertoire appears to be shaped by both extrinsic and intrinsic factors (Kenny et al., 1983; Briles et al., 1981; Mi et al., 2000; Kearney et al., 2015; Patel and Kearney, 2015; Kreuk et al., 2019; Zeng et al., 2018; New et al., 2020). In mice, nIgM has been shown to originate largely from differentiated, self-reactive B-1 cells that appear to require no foreign antigen stimulation to induce nIgM secretion (Baumgarth et al., 2000; Lalor et al., 1989; Choi et al., 2012; Kantor and Herzenberg, 1993) and that escape negative selection during fetal and early neonatal life (Hayakawa et al., 2003; Hayakawa et al., 1999). Additionally, some nIgM may also be produced by marginal zone B cells (Ichikawa et al., 2015), although the extent to which they contribute to the overall nIgM pool has not been assessed. A recent study proposed that a non-identified B cell population in the body cavity, distinct from that of B-1 cells, might be the source of IgM-secreting BM plasma cells (PCs) as purified body cavity B-1 cells when transferred to T and B cell–deficient $Rag^{-/-}$ mice did not reconstitute serum IgM levels, while the transfer of total body cavity wash-out cells did (Reynolds et al., 2015).

Consistent with previous studies identifying the spleen and BM as major sites of IgM production, we demonstrated that nIgM-secreting B-1 cells are located mainly in the spleen and BM (Choi et al., 2012; Savage et al., 2017). Furthermore, we demonstrated the presence of two distinct populations of B-1 cell–derived cells secreting nIgM: non-terminally differentiated B-1 cells ($B\text{-}1_{sec}$; $Dump^-$, $CD23^-$, IgD^-, $CD43^+$, $CD19^+$, and IgM^+) that generated IgM even in the apparent absence of the transcriptional regulator of PC development, BLIMP-1 (Shapiro-Shelef et al., 2003), and terminally differentiated BLIMP-1^+ B-1–derived PCs (B-1PC; $Dump^-$, $CD23^-$, IgD^-, $CD43^+$, $CD19^{lo/neg}$, IgM^+, CD138, and/or Blimp-1^+). The latter was estimated to secrete about two-thirds of the circulating serum nIgM (Savage et al., 2017). The presence of two distinct nIgM-secreting cell types suggested that nIgM-secreting B-1PC and $B\text{-}1_{sec}$ might be induced by distinct activation pathways and may also differ from the non-secreting B-1 cells in the body cavities.

Studies shown here further support the B-1 origins of IgM-secreting BM and splenic PCs and demonstrate that BM, but not spleen B-1PC, require the presence of $\alpha\beta TCR^+$ $CD4^+$ T cells for their development. B-1PC generate a highly oligoclonal repertoire of nIgM with unique characteristics that differ sharply from those previously associated with B-1 cell–derived nIgM.

Results

nIgM-secreting B-1PC appear in BM and spleen over time

Most spontaneous IgM-ASC in the BM and spleen of C57BL/6 mice are B-1 cell–derived and consist of non-terminally differentiated $B\text{-}1_{sec}$ and terminally differentiated B-1PC (Savage et al., 2017). These two cell populations are distinguished by their phenotype. $B\text{-}1_{sec}$ are present in small frequencies among "classical" B-1 cells ($CD19^{+/int}$ IgM^{hi} IgD^{lo} $CD23^-$ $CD43^+$) in BM and spleen, while B-1PC are distinguished from these cells as being $CD19^{lo/neg}$ IgM^+ IgD^{lo} $CD138^+$ (Savage et al., 2017; Choi et al., 2012). Thus, B-1PC phenotypically resemble conventional, B-2 cell–derived PC. Most B-1PC also expressed the transcriptional regulator Blimp-1, and virtually every cell spontaneously secreted IgM when deposited into an ELISPOT plate (Fig. 1, A and B; Savage et al., 2017). Measuring the appearance of B-1 and B-1PC in ontogeny revealed that, as expected, B-1 cells were present in the spleen and BM at birth, with frequencies reaching those seen in adult mice by about postnatal day 18. In contrast, B-1PC were absent in neonates and did not emerge until mice reached 3–4 wk of age (Fig. 1, A, C, and D). Their appearance correlated with a rapid increase in serum IgM (Fig. 1 E), consistent with their previously noted significant contributions to nIgM production (Savage et al., 2017; Savitsky and Calame, 2006). The frequency and number of B-1PC in spleen and BM of germ-free mice was similar to that of mice held under SPF conditions (Fig. 1 F), consistent with data showing that serum IgM concentrations are similar in SPF-held and germ-free mice (Bos et al., 1989; Haury et al., 1997), although microbiota may alter their specificity (Kreuk et al., 2019; New et al., 2020). It appeared thus unlikely that the delayed development of B-1PC was due to a need for microbial antigen and/or pathogen-associated molecular pattern–induced B-1 cell differentiation.

Early adoptive cell transfer studies showed that B-1 cells develop predominantly during fetal and early neonatal life and rely on a transcriptional gene network epigenetically regulated by Lin28/Let7 (Hayakawa and Hardy, 2000; Yuan et al., 2012; Li et al., 2015). Furthermore, the use of an irreversible lineage tracing model, the FlkSwitch mouse, revealed the presence of two distinct fetal hematopoietic stem cell (HSC) populations giving rise to B-1 cells: a transient, developmentally restricted (dr) HSC population in the fetal liver, which preferentially gives rise to innate lymphoid lineage cells only during a distinct window in fetal development, and a population of long-term fetal liver and BM HSC that generate both innate-like and conventional lymphocytes (Beaudin et al., 2016). In this model, the fetal liver drHSC can be distinguished from the long-term reconstituting fetal-derived HSC by their early Flk-induced expression of GFP, instead of Tomato Red (Tom), although some contamination of Tom+HSC by drHSC cannot be excluded (Boyer et al., 2012; Boyer et al., 2011; Beaudin et al., 2016). All daughter cells eventually express GFP due to the induction of Flk later in B cell differentiation (Boyer et al., 2011). We used this lineage tracing model, studying lethally irradiated adult recipients that were reconstituted with either of the two purified HSC populations (Fig. 1 G), to determine whether the later

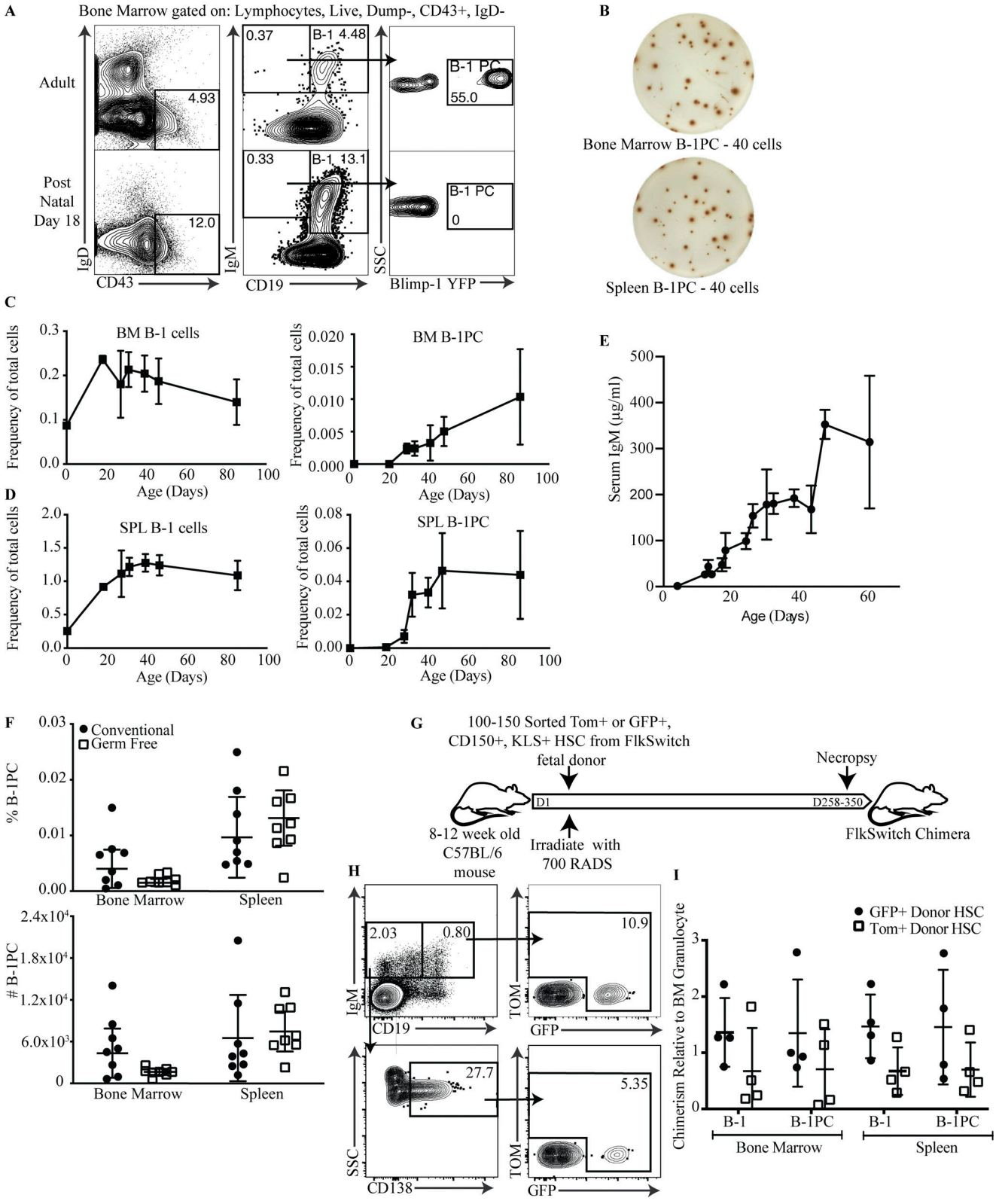

Figure 1. **nIgM-secreting B-1 PC in BM and spleen appear over time. (A)** Representative FACS plots of BM from adult and postnatal day 18 Blimp-1 YFP reporter mice showing gating for B-1 cells (IgD$^-$, CD43$^+$, IgM$^+$, CD19^{hi}) and B-1 PCs (IgD$^-$, CD43$^+$, IgM$^+$, CD19$^{neg/lo}$ Blimp-1 YFP$^+$). **(B)** Representative IgM ELISPOTs by B-1PC in BM and spleen of adult Blimp-1 YFP mice; number of cells sorted into each well are indicated. **(C and D)** Mean percent ± SD B-1 cells and B-1PCs in BM (C) and spleen of mice at indicated ages (D; n = 3–6 mice per age group for days 18–85, n = 2 for day 0). SPL, spleen. **(E)** Mean ± SD serum IgM (µg/ml), determined by ELISA, in mice at indicated ages (n = 3–6 mice per age group). **(F)** Mean percent ± SD live (top) and total number B-1PC in BM and spleen (bottom) of SPF versus germ-free held mice (n = 8 mice/group). Symbols are results from one mouse. Data are combined from two independent experiments. **(G)** Schematic of FlkSwitch chimera generation protocol. **(H)** Representative FACS plots of HSC marker presence among B-1 and B-1 PCs in BM of mice

reconstituted with FACS-purified transient fetal drHSC (GFP+) or conventional fetal (TdTomato+) HSC, respectively. **(I)** Mean relative percent B-1 and B-1 PC in spleen and BM expressing HSC markers compared with BM granulocytes (n = 4 GFP [drHSC], n = 4 TdTomato [conventional fetal HSC]). Values in H were compared using a one-way ANOVA. Values in F were compared by unpaired Student's t test.

appearance of B-1PC was due to B-1PC precursors emerging only from the later appearing HSCs. B-1PC were found in mice reconstituted with both drHSC and Tom+HSC. Compared to the development of granulocytes, the B-1PC compartment was preferentially reconstituted by the early-arising drHSC, and thus is similar to the preferential reconstitution of B-1 cells (Fig. 1, H and I). Thus, while B-1PC precursors are present already in the fetus and the neonate, B-1PC differentiation is delayed until around the time of weaning.

The development of BM B-1PC requires the presence of T cells

Although natural antibody production is widely reported to occur independent of T cells, adoptive transfer of B-1 cells into B and T cell–deficient $Rag^{-/-}$ mice showed relatively poor reconstitution of BM IgM production and total serum IgM levels (Moon et al., 2004; Reynolds et al., 2015). In contrast, adoptive transfer of total peritoneal cavity wash out or of peritoneal cavity B-1 cells into B cell–deficient and T cell–sufficient neonates resulted in robust nIgM reconstitution (Savage et al., 2017; Baumgarth et al., 1999; Stall et al., 1992). Interestingly, depletion of T cells from peritoneal cavity cells prior to transfer into newborn mice also was reported to reduce serum IgM levels compared with total peritoneal cavity wash-out transfers (Förster and Rajewsky, 1987), suggesting that the difference in serum IgM reconstitution was not dependent on the age of the B-1 cell recipients. We, therefore, reconsidered the role of T cells in nIgM production and B-1PC development and studied B-1PC populations in adult T cell–deficient $TCR\beta/\delta^{-/-}$ mice (Mombaerts et al., 1992). Indeed, these mice showed a near complete lack of BM B-1PC (Fig. 2, A and B), while the splenic B-1PC compartment appeared largely unaffected (Fig. 2 C).

Despite the absence of BM B-1PC, and consistent with previous studies (Hooijkaas et al., 1985; Van Oudenaren et al., 1984; Madsen et al., 1999), the number of nIgM ASC in the BM of adult $TCR\beta/\delta^{-/-}$ mice and their serum IgM levels were comparable with T cell containing control mice (Fig. 2, D and E). This was explained by a striking increase in the frequency and number of B-1 cells in both BM and spleen of $TCR\beta/\delta^{-/-}$ mice (Fig. 2, B and C, lower panels), the subset that contains nIgM-secreting $B\text{-}1_{sec}$ cells (Savage et al., 2017). Furthermore, measuring serum IgM concentrations during early life showed that $TCR\beta/\delta^{-/-}$ mice had transiently reduced IgM concentrations between 3 and 5 wk of age compared with controls (Fig. 2 E), the age at which the BM B-1PC compartment rapidly expanded (Fig. 1, A and B). Serum IgM concentrations in the $TCR\beta/\delta^{-/-}$ mice reached levels comparable with that of the controls by about 8 wk of age (Fig. 2 E). The data suggest that nIgM-secreting BM B-1PC, but not spleen B-1PC or $B\text{-}1_{sec}$, require the presence of T cells for development. The apparent normal nIgM concentrations in the serum of $TCR\beta/\delta^{-/-}$ mice seemed to be restored, at least in part, via compensatory increases in BM $B\text{-}1_{sec}$ cell differentiation and/or maintenance.

Establishment of BM B-1PC requires CD4 T cells

Long-lived conventional B cell–derived Blimp-1^+ PCs require costimulatory signals from CD4 T cells (Gershon, 1974; Keightley et al., 1976). Consistent with these findings, the depletion of $CD4^+$ cells from newborn C57BL/6 mice via anti-CD4 mAb treatment (GK1.5) resulted in greatly reduced numbers of IgM^+ BM B-1PC (Fig. 3, A and B) but did not significantly affect serum IgM concentrations (Fig. 3 C). We also depleted CD4 T cells from neonatal Ig-allotype chimeras by treating Igha-expressing C57BL/6 mice with anti-CD4 mAb. In addition, these neonatal chimeras were rendered host B cell–deficient from birth until 6 wk of age via treatment with allotype-specific anti-IgM (Igh-a). To replace their B-1 cell compartment, these mice were reconstituted, also at birth, with body cavity B-1 cells from allotype-disparate (Igh-b) but congenic adult C57BL/6 mice (Fig. 3 D). Body cavity cells can reconstitute the host B-1 cell but not the B-2 cell compartment, as the anti-IgMa treatment does not affect their presence and B-2 cells do not survive the transfer (Lalor et al., 1989; Förster and Rajewsky, 1987). This enables tracing of B-1 and B-2 cell–derived serum IgM via their expressed Ig-allotype (Baumgarth et al., 1999; Förster and Rajewsky, 1987). Antibody-mediated CD4 cell depletion greatly reduced the numbers of BM Igh-b^+ B-1PCs compared with control Ig-allotype chimeras that had received PBS only (Fig. 3, E and F). The data further confirmed the B-1 cell origin of the BM IgM^+ PC and demonstrated their dependence on CD4 T cells for development.

The compensatory increases in BM and spleen B-1 cell numbers seen in the $TCR\beta/\delta^{-/-}$ mice were not seen in the CD4-depleted neonatal Ig-allotype chimeras. In fact, a significant drop in BM B-1 cell frequency and total numbers was seen (Fig. 3 F, lower panels) in a population that contains nIgM secreting $B\text{-}1_{sec}$ (Savage et al., 2017). Consistent with reductions of both nIgM-secreting B-1 cell populations, CD4-depleted Ig-allotype chimeras had severely reduced concentrations of serum IgM compared with the controls (Fig. 3 G). This failure to compensate for the depletion of BM B-1PC by $B\text{-}1_{sec}$ in chimeras in which all B-1 cells are reconstituted by adult-type body cavity B-1 cells may suggest that this functionality is restricted to fetal/neonatal B-1 cells and/or B-1 cells that reside outside the body cavities. The data indicate that functional heterogeneity exists within the B-1 cell compartment, a finding that requires future exploration.

Maintenance of B-1PC does not require CD4 T cells

It was shown recently that $CD4T_{regs}$ create a niche in BM that supports the survival of PC (Glatman Zaretsky et al., 2017). To determine whether CD4 T cells are required for the development or maintenance of B-1PC in the BM, adult mice were depleted of all CD4 T cells via anti-CD4 mAb treatment for 56–72 d (Fig. 4 A). In contrast to neonatal anti-CD4 treatment, there was no effect on the frequency or number of BM B-1PC in adult anti-CD4 treated mice compared with their controls (Fig. 4 B) nor was

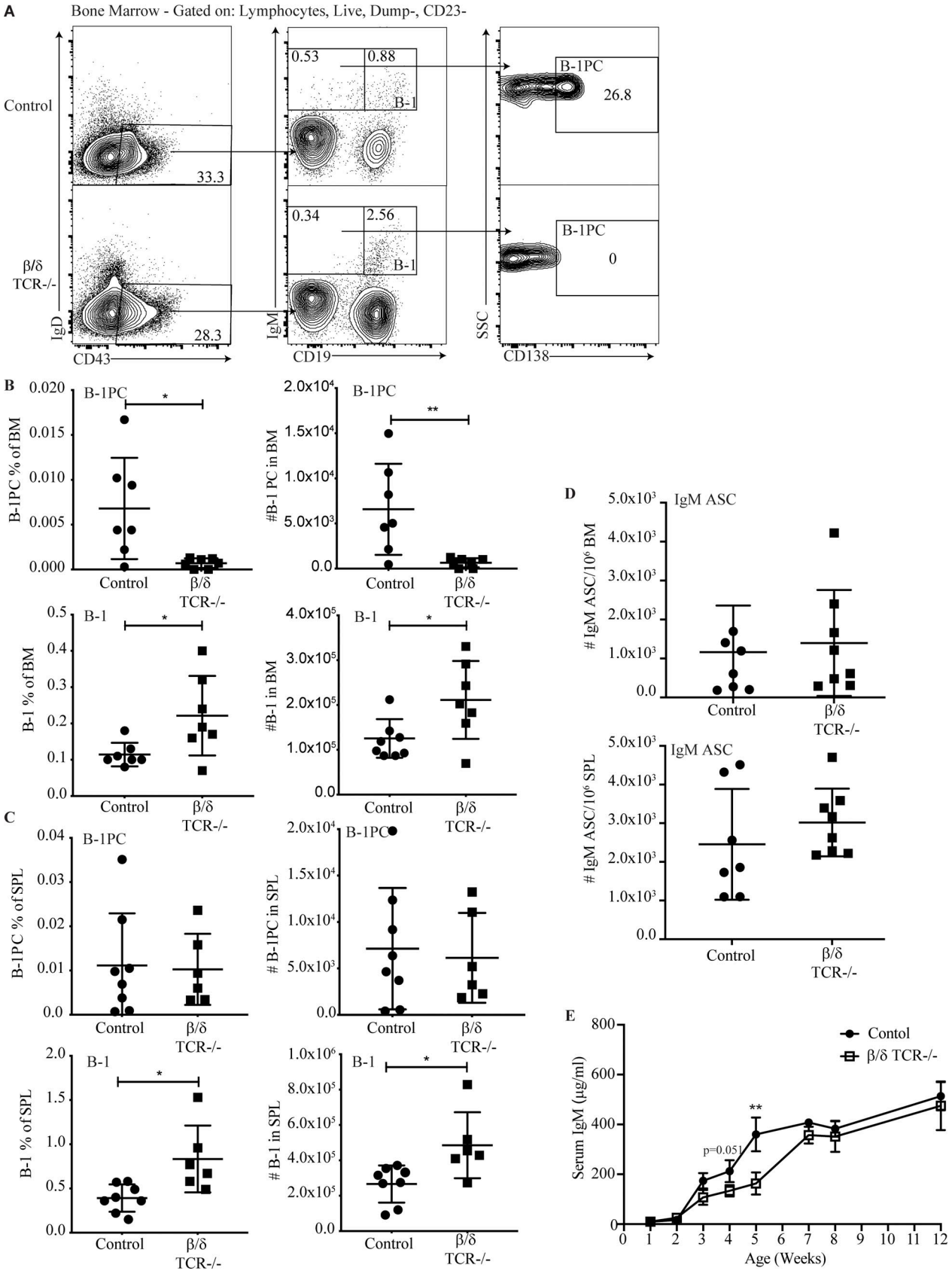

Figure 2. **BM B-1PC requires T cells. (A)** Representative FACS plots of live, singlet, Dump⁻ CD23⁻ BM from C57BL/6 (control) and complete β/δ TCR$^{-/-}$ mice. **(B and C)** Mean percentage ± SD (left) and total numbers (right) of B-1PC and B-1 cells as indicated, in (B) BM and (C) spleen. *n* = 6–8/group; symbols represent data from individual mice. SPL, spleen. **(D)** Mean number ± SD BM IgM ASC per 10^6 total cells in BM (top) and spleen (bottom); *n* = 7–8/group. **(E)**) Mean ± SD serum IgM (μg/ml) in control and β/δ TCR KO mice; *n* = 4–6 mice per time point. Data in B–E are combined from two independent experiments. Values in B, C, and D were compared by unpaired Student's *t* test. *, 0.01 ≤ P < 0.05; **, 0.001 ≤ P <0.01.

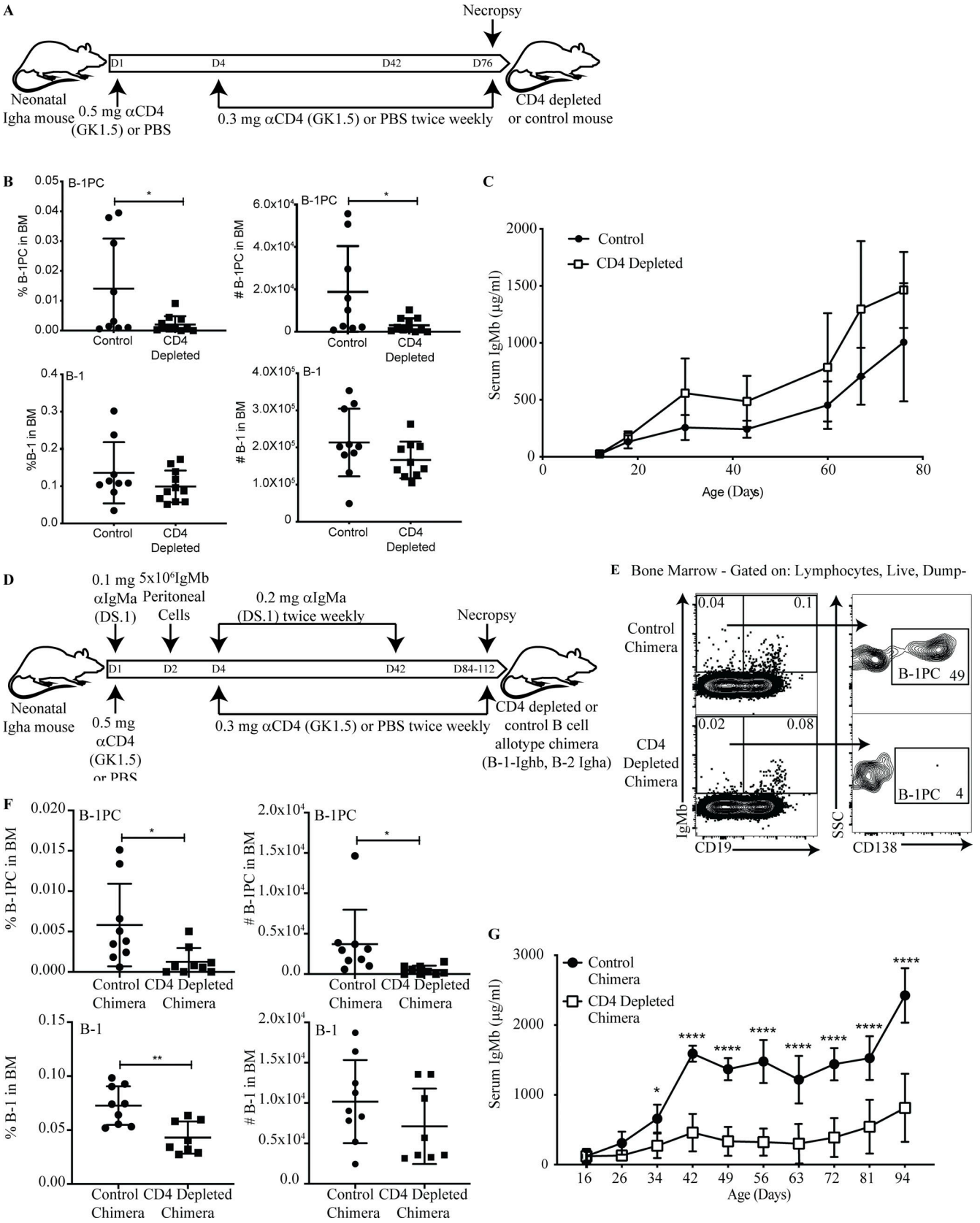

Figure 3. **BM B-1 PC establishment requires CD4⁺ T cells. (A)** Experimental layout of CD4 depletion in neonatal mice. **(B)** Mean percent ± SD live cells (left) and total number (right) of BM B-1PCs (top) and B-1 cells (bottom) in C57BL/6 mice treated from birth with PBS (control) or anti-CD4 mAb (GK1.5; CD4 depleted); *n* = 9–11/group. Each symbol represents an individual mouse. **(C)** Mean ± SD serum IgM (μg/ml) in control and CD4-depleted mice (*n* = 4–7 per time point). **(D)** Experimental layout for the generation of neonatal B cell allotype chimeras with/without CD4 depletion. **(E)** Representative gating strategy for B-1 PCs

(IgMa$^-$, IgMb$^+$, CD19$^{neg/lo}$, CD138$^+$) and B-1 cells (IgMa$^-$, IgMb$^+$, CD19^{hi}) in B cell Ig-allotype chimera treated from birth with PBS (control) or with anti-CD4 (CD4-depleted chimera). **(F)** Mean percent ± SD live cells (left) and total number (right) of B-1PCs (top) and B-1 cells (bottom) in BM. **(G)** Mean ± SD serum IgMb (µg/ml) in chimeras as in E (n = 9 per time point, except day 94 n = 4). Data in B, C, E, and F are pooled from two independent experiments. Values in B and F were compared by unpaired Student's t test. Values in C and G were compared using two-way repeats measure ANOVA with post hoc multiple comparison. *, 0.01 ≤ P < 0.05; **, 0.001 ≤ P < 0.01; ****, 0.00001 ≤ P < 0.0001.

there any difference in their serum IgM levels or numbers of BM IgM ASCs (Fig. 4, C–E). Treatment of fully reconstituted adult Ig-allotype chimeras confirmed that IgM$^+$ B-1–derived PC frequencies and numbers and serum IgM concentrations were not affected by CD4 depletion (Fig. 4, F and G). Together, the data show that CD4 T cells are required for the induction but not maintenance of the BM IgM$^+$ B-1PC pool.

CD4$^+$ T cells are sufficient to rescue BM B-1PC development

To directly assess whether purified B-1 cells could reconstitute the B-1PC compartment in the presence of CD4 T cells, we reconstituted neonatal T and B cell–deficient Rag1$^{-/-}$ mice with either MACS-enriched peritoneal cavity B-1 cells alone or together with highly MACS-enriched splenic CD4 T cells (Fig. 5 A). FACS analysis of mice aged 112 days demonstrated that CD4 T cells were both necessary and sufficient for PC development from purified B-1 cells (Fig. 5 B and C). Consistent with previous studies (Förster and Rajewsky, 1987; Reynolds et al., 2015), mice reconstituted with B-1 cells alone in the absence of T cells had low numbers of IgM ASC in the BM (Fig. 5, D and E) as well as low concentrations serum IgM (Fig. 5 F). However, the co-transfer of CD4$^+$ T cells allowed purified B-1 cells to reconstitute the pool of IgM-secreting BM PCs, consistent with results in the Ig-allotype chimeras (Fig. 3 E), where B-1 cells reconstituted nIgM and B-1PC unless they were depleted of CD4 T cells. This was confirmed by reconstituting adult T and B cell–deficient Rag1$^{-/-}$ mice with either highly pure populations (>98%) of FACS-sorted peritoneal cavity B-1 cells alone or together with highly pure (>98%) FACS-sorted splenic CD4 T cells, or with FACS-sorted peritoneal cavity cells depleted of B-1 cells but containing CD4 T cells (Fig. 5 G). Results demonstrated that B-1PC formation requires both, B-1 cells and CD4$^+$ T cells (Fig. 5, H–L). Mice that received only B-1 cells had very low numbers of IgM ASC in the BM compared to B-1 cells transferred with CD4$^+$ T cells (Fig. 5, H–J). In addition, mice receiving total peritoneal cells, including CD4 T cells, but depleted of B-1 cells also failed to produce significant numbers of BM IgM ASC, while those receiving both B-1 and CD4 T cells showed robust, albeit variable, BM B-1PC development (Fig 5, H–J). In addition, serum IgM levels were very low in those recipients that received either B-1 cells alone or peritoneal cells depleted of B-1 cells compared with mice given B-1 cells plus CD4$^+$ T cells 7 wk after cell transfer (Fig. 5 K). Of note, serum IgM levels did not begin to rise for about 3 wk after transfer of B-1 and CD4 T cells (Fig. 5 K), a timeline similar to the one noted for non-manipulated neonatal wild type mice (Fig. 1). The functional importance of the B-1PC was further indicated by showing that serum IgM levels were significantly and positively correlated with the number of BM B-1PC (Fig. 5 L), the latter assessed by flow cytometry.

Conventional B cells receive T cell help from CD4$^+$ TCRαβ$^+$ MCH II-restricted T cells to generate long-lived BM PC (Noelle et al., 1992), while glycolipid-specific CD1d-restricted invariant (i) natural killer T (NKT) cells, as well as TCRγδ$^+$ T cells, were shown to provide cytokine-mediated "help" to B-1 cells in inflammation and infection (Campos et al., 2006; Wang et al., 2016). Yet, mice deficient in TCRαβ$^+$ cells (Fig. 6 A) and neonatal Ig-allotype chimeras reconstituted with total peritoneal cavity wash-out and depleted of all TCRαβ$^+$ T cells via treatment with an anti-pan-TCRαβ mAb (H57-597.1) that depletes all endogenous, as well as adoptively transferred T cells (Fig. 6 B), but not mice deficient in γ/δ T cells (Fig. 6 C) or CD1d-restricted T cells (Fig. 6 D) had greatly reduced B-1PC compartments, similar to those seen after anti-CD4 treatment (Fig. 3, D–F). Similarly, MHCII-deficient mice, lacking TCRαβ$^+$ CD4 T cells, showed strong reductions in BM B-1PC numbers (Fig. 6 E). Together, the data demonstrate that BM B-1PC accumulation and nIgM secretion by these cells is dependent on the presence of MHCII-restricted TCRαβ$^+$ CD4 T cells.

T cell–driven development of BM B-1 PC occurs in a non-cognate, CD40L- and IL-5–independent manner

Peptide/MHCII–TCR cognate interaction between CD4$^+$ T cells and B-2 cells is required for the development of conventional PC against T-dependent antigens (Ise and Kurosaki, 2021). While B-1 cells are considered to be involved in T-independent responses, they can stimulate antigen-specific CD4$^+$ T cell responses (Margry et al., 2013; Zimecki and Kapp, 1994; Zimecki et al., 1994). Using the Rag1$^{-/-}$ reconstitution model (Fig. 5 A), we show that the relative and total number of B-1PC, and the numbers of IgM ASCs and serum IgM concentrations were unaffected in mice given MCHII-deficient B-1 cells and splenic CD4 T cells (Fig. 7, A–C).

The presence of IL-5 has been shown to increase CD5$^+$ B-1 cell numbers in the peritoneal cavity of preweaned mice (Kopf et al., 1996) and enhance serum IgM levels (Moon et al., 2004; McKay et al., 2017). ILC-2–derived IL-5 was shown also to enhance B-1 cell–derived IgM responses to infection (Jackson-Jones et al., 2016). In support, stimulation of peritoneal cavity B-1 cells with IL-5 alone induced IgM production, whereas stimulation with IL4 (data not shown) and CD40L failed to do so (Fig. 7 D). However, neither CD40L$^{-/-}$ nor IL-5$^{-/-}$ mice showed significant differences in numbers or frequencies of BM B-1PC (Fig. 7, E and G) or the number of IgM ASC (Fig. 7, F and H). Furthermore, reconstitution of Rag$^{-/-}$ mice with purified B-1 cells and CD4 T cells from IL-5$^{-/-}$ or control C57BL/6 mice showed no difference in the frequency or number of BM B-1PC (Fig. 7 I) or BM IgM ASC (Fig. 7 J). We conclude that BM B-1PC develop independently of cognate CD4 T cell–B-1 cell interaction and do not require IL-5 production by CD4 T cells.

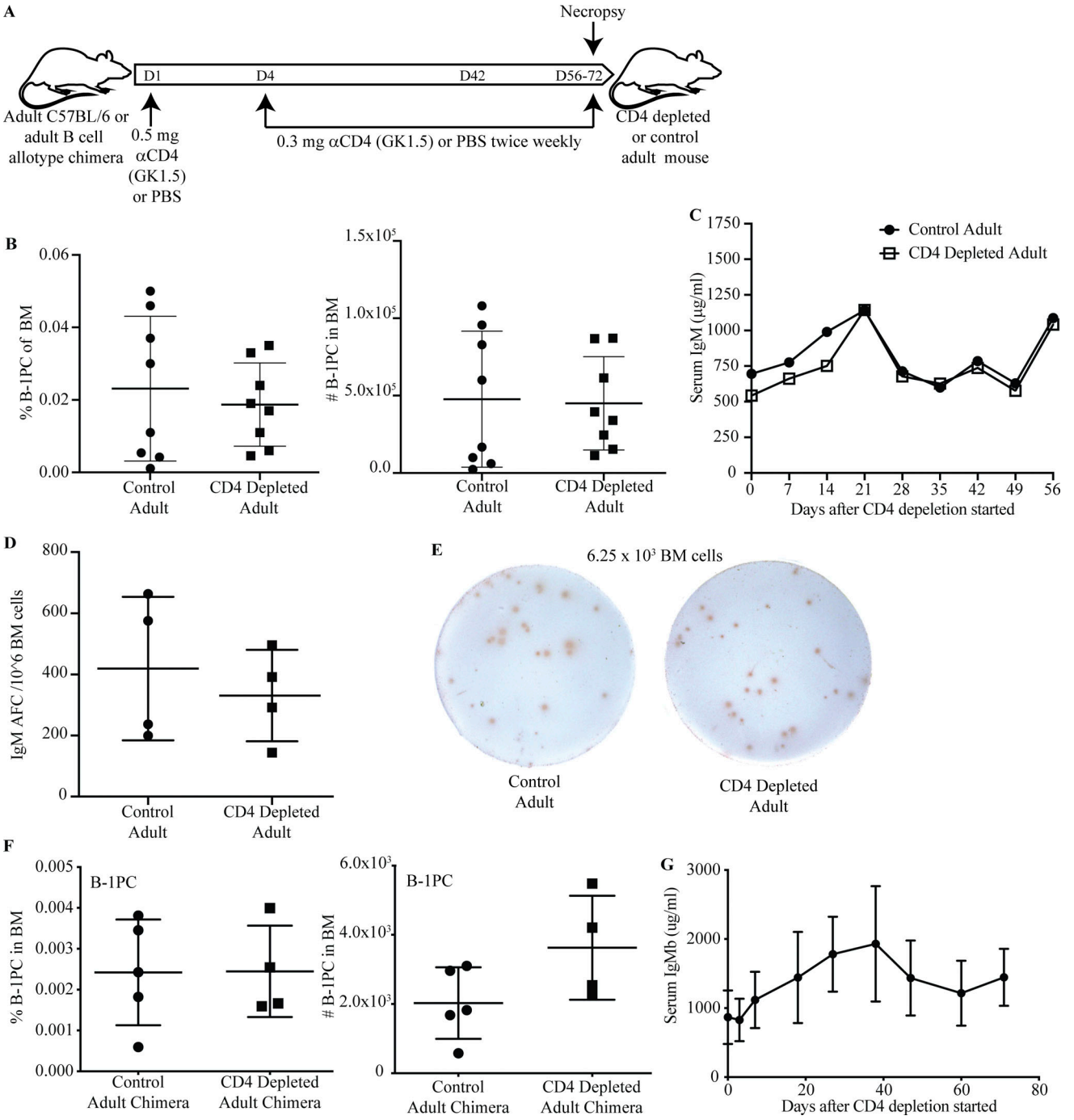

Figure 4. **BM B-1 PC maintenance does not require CD4⁺ T cells. (A)** Experimental layout of CD4 depletion in adult C57BL/6 mice or adult B cell allotype chimeras. **(B)** Mean percent ± SD of live cells (left); and total number (right) of B-1PCs in BM of untreated or anti-CD4–treated adult C57BL/6 mice treated from the age 56 d to analysis (n = 8/group). **(C)** Mean ± SD serum IgM (μg/ml) in mice from B during CD4 depletion. **(D)** Mean number ± SD IgM ASC per 10^6 total cells in BM of adult CD4-depleted mice and controls from (B). **(E)** Representative IgM ELISPOTS of mice in B. **(F)** Mean percent ± SD of live cells (left) and total number (right) of B-1PCs in BM of untreated or anti-CD4–treated adult allotype chimeras treated from age 84 d to analysis (n = 4–5/group). **(G)** Mean ± SD serum IgMb (μg/ml) in adult treated chimeras and controls from F (n = 4 per time point). Data in B are pooled from two independent experiments. Values in B, D, and F were compared by unpaired Student's t test. Values in C and G were compared using two-way repeats measure ANOVA for differences between groups and time points with post hoc multiple comparison.

B-1 and B-1PC express Ig of distinct specificities

We next asked whether B-1PC and B-1_{sec} differed in the nIgM specificities they generate. Roughly 5–15% of peritoneal cavity CD5⁺ B-1 cells and 1–10% of spleen B-1 cells bind liposomes containing phosphatidylcholine (PtC; Carmack et al., 1990; Mercolino et al., 1988; Hayakawa et al., 1992). The relative concentration of anti-PtC–specific serum IgM, however, was found to be very low (Goodridge et al., 2014). Thus, the

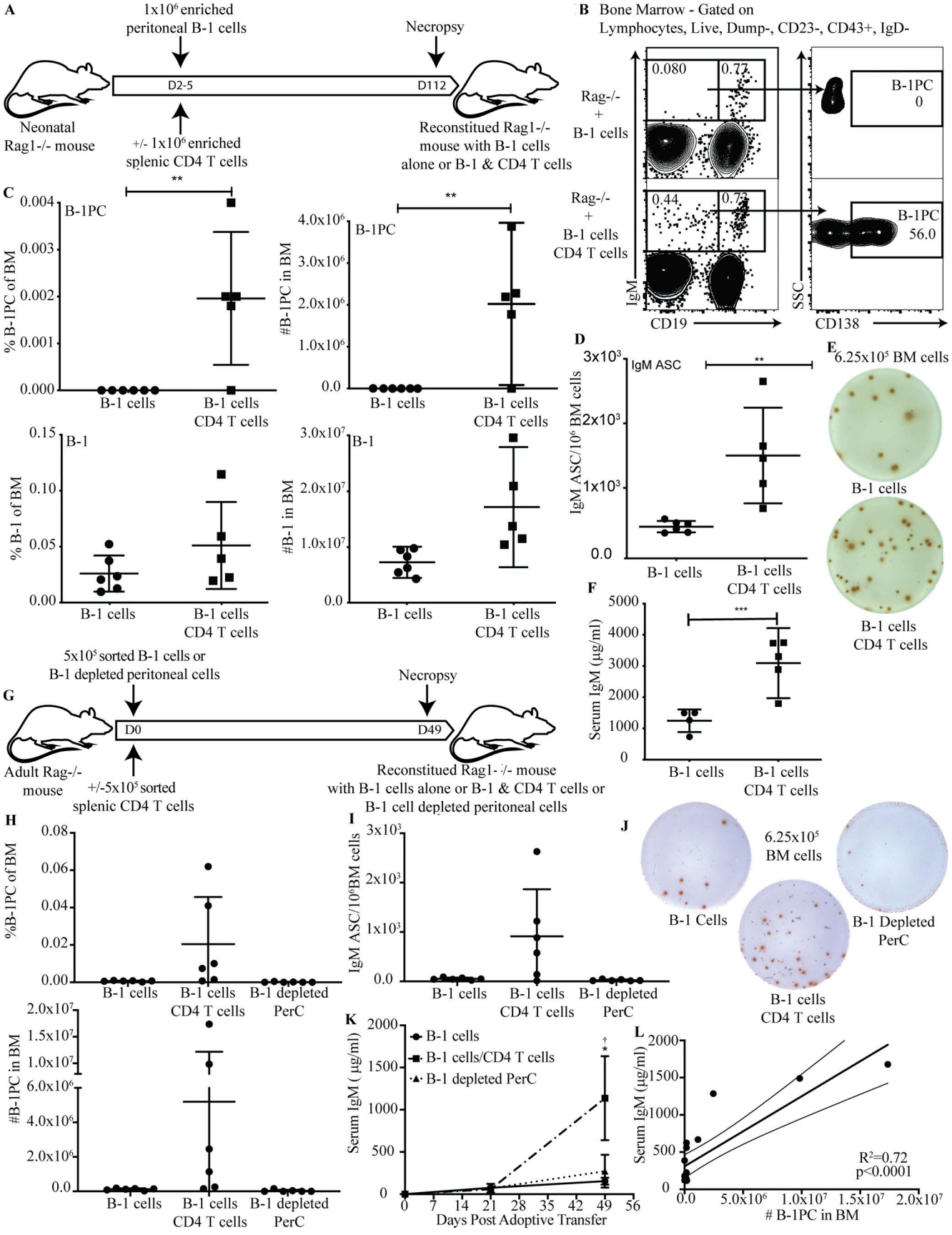

Figure 5. **CD4⁺ T cells are sufficient to rescue BM B-1 PC development. (A)** Experimental layout of Rag1$^{-/-}$ mouse reconstitution with B-1 cells alone or B-1 + splenic CD4⁺ T cells. **(B)** Representative FACS plots of BM from Rag1$^{-/-}$ mice reconstituted on postnatal day 2 with peritoneal B-1 alone or peritoneal B-1 and

splenic CD4+ T cells. Gating identifies B-1 cells (IgD−, CD43+, IgM+, CD19hi) and B-1 PCs (IgD−, CD43+, IgM+, CD19neg/lo, CD138+). **(C)** Mean percent ± SD live cells (left) and total number (right) of B-1PCs (top) and B-1 cells (bottom) in BM in mice from B (n = 5–6/group). **(D)** Mean number ± SD BM IgM ASC per 10^6 total cells (n = 5–6/group). **(E)** Representative ELISPOTs of IgM ASC from BM. **(F)** Mean ± SD serum IgM (μg/ml) at 16 wk of age (n = 5–6/group). **(G)** Experimental layout of adult Rag1−/− mouse reconstitution with B-1 cells alone or B-1 + splenic CD4+ T cells or peritoneal cells depleted of B-1 cells. **(H)** Mean percent ± SD live cells (top) and total number (bottom) of B-1PC by FACS in BM in mice given FACS-sorted B-1 cells only, B-1 cells + CD4 T cells, or B-1 cell–depleted peritoneal cells (n = 6/group). **(I)** Mean number ± SD BM IgM ASC per 10^6 total cells (n = 6/group). **(J)** Representative ELISPOTs of IgM ASC from BM. **(K)** Mean ± SD serum IgM (μg/ml) at 0, 21, and 49 d after adoptive transfer (n = 6/group). **(L)** Correlation between the number of BM B-1PC as determined by FACS and serum IgM (μg/ml) at 49 d after adoptive transfer. All data were pooled from two independent experiments. Values in C, D, and F were compared by unpaired Student's t test. Values in H and I were compared by a one-way ANOVA with post hoc testing for multiple comparison, and K was compared by a two-way ANOVA with post hoc testing for multiple comparison. *†, 0.01 ≤ P < 0.05; **, 0.001 ≤ P < 0.01; ***, 0.0001 ≤ P < 0.001.

repertoire of serum nIgM does not seem to reflect that of the non-secreting body cavity B-1 cells nor the overall splenic CD5+ B-1 cell compartment. Indeed, while about 0.4% of B-1 cells in BM and 5% of spleen B-1 cells bound to PtC liposomes in our studies, a small fraction of which may include B-1_{sec} (Savage et al., 2017), B-1PC in both the spleen and BM showed no binding to these liposomes despite high levels of surface IgM expression (Fig. 8, A and B). Additionally, flow cytometric depletion of B-1 cells (CD19int/hi IgMhi), but not B-1PC (CD19lo/neg, IgM+, CD138+, Blimp-1+), from CD43+ IgM+ BM B cells resulted in significant reductions in the frequencies of anti-PtC IgM ASCs (Fig. 8, C and D). Thus, anti-PtC nIgM ASC appear to be among B-1_{sec} but not B-1PC.

B cell receptors (BCR) encoded by Ig heavy chain variable regions VH11 and VH12 are largely restricted to the CD5+ B-1 cell compartment and include cells with specificity for PtC (Conger et al., 1991; Arnold and Haughton, 1992). Consistent with the distribution of the PtC-binders among B-1_{sec} but not B-1PC (Fig. 8, A and B), the frequencies of VH11- and VH12-expressing cells were higher among peritoneal cavity B-1 cells compared with splenic or BM B-1 cells, and almost completely absent from the spleen and BM B-1PC (Fig. 8 E). Similarly, B-1 cell–derived nIgM to phosphorylcholine (PCh), which is protective against infections with *S. pneumoniae* (Briles et al., 1981), was mostly secreted by B-1_{sec} in the spleen, but not the BM, with some secretion by splenic B-1PC (Fig. 8 F). Consistent with a lack of PCh-specific IgM BM B-1PC, PCh-specific IgM serum levels were comparable between control and TCRβδ−/− mice (Fig. 8 G), confirming the T cell independence of anti-PCh antibodies (Haas et al., 2005). In contrast, influenza virus–binding nIgM was secreted almost exclusively by B-1PC in both spleen and BM (Fig. 8, H and I) and their levels were significantly reduced in TCRβδ−/− mice, consistent with the noted T cell-dependence of the B-1PC compartment (Fig. 8 J). Autoantigen-specific serum IgM measured against a broad array of autoantigens showed no difference between wild type control mice and mice that lacked T cell-dependent BM B-1PC, including TCRβ/δ−/− mice, CD4+ depleted Ig-allotype chimeras, and B-1 cell reconstituted Rag1−/− mice (Fig. S1). The data indicate that B-1PC do not contribute significantly to the production of strongly autoreactive nIgM.

B-1PC express a highly oligoclonal, germline-encoded Ig repertoire

To assess the repertoire of B-1PC, we separately sequenced the Ig-heavy chains (Igh) from bulk RNA of 3,000 flow cytometry-purified spleen and BM CD5+ and CD5− B-1 cells, B-1PC as well as CD23+ mature, naive conventional B cells from four individual mice. The data further supported our conclusion that B-1_{sec} and B-1PC secrete distinct nIgM. Overall, B-1PC showed little Igh-repertoire overlap with either CD5+ B-1, CD5− B-1, or conventional B cells isolated from the same tissue (Fig. 9, A and B). The exception was mouse 2, which showed a much higher degree of overlap between CD5− B-1 and B-1PC in the BM (Fig. 9, A and B) compared with the other mice. This mouse also expressed the most oligoclonal repertoire of the mice examined (Fig. 9 A). Thus, based on the repertoires, it appears that the B-1PC expand from overall rare specificities found in the peripheral B-1 cell compartments. To study the repertoire overlaps, we determined the Morisita Overlap Index for each of the sorted cell populations. Using a measure of 0 for no overlap to 1 of complete overlap, the results demonstrate that while the repertoires of BM and spleen B-1PC from the same mouse overlapped to a certain degree, ranging from 0.13 to 0.68, no consistent overlap was found between B-1PC and other B cells populations within one mouse, and between mice (Fig. S2). An acknowledged limitation of our assays is that the repertoire of the non-secreting cells may not have been assessed as comprehensively as that of the B-1PC due to the much lower number of Ig-transcripts.

B-1PC were uniformly marked by a high degree of Igh-repertoire oligoclonality. About 70% of the Igh variable repertoire of BM B-1PC was encoded by between 1 and 10 unique CDR3 Igh sequences per mouse (Fig. 9 A) Among spleen B-1PC, about half of the CDR3 regions were encoded by between 1 and 20 unique sequences (data no shown). Thus, extensive clonal expansion seemed to have preceded B-1PC differentiation. Furthermore, the level of oligoclonality exceeded that of both the CD5+ and CD5− B-1 cells (Fig. 9 A), which had been shown previously to contain expanded clones and a repertoire that is less diverse than that of conventional B cells (Yang et al., 2015; Prohaska et al., 2018; Upadhye et al., 2019). B-1PC have a mutation rate of 2.3% and 1.7% in BM and spleen, respectively (Fig. 9 C), and while there are significant differences between almost all the populations of B-1 cells, in general, these low mutation rates are consistent with fetal/neonatal origins and are lower than what is reported for antigen-induced IgM PCs (Bohannon et al., 2016).

B-1PC express a unique, public repertoire with short junctional sequences

In contrast to the other B cell populations studied, B-1PC contained a predominance of clones with short junctional length (7–8 aa; Fig. 10, A and B). The junctional sequences encoding the

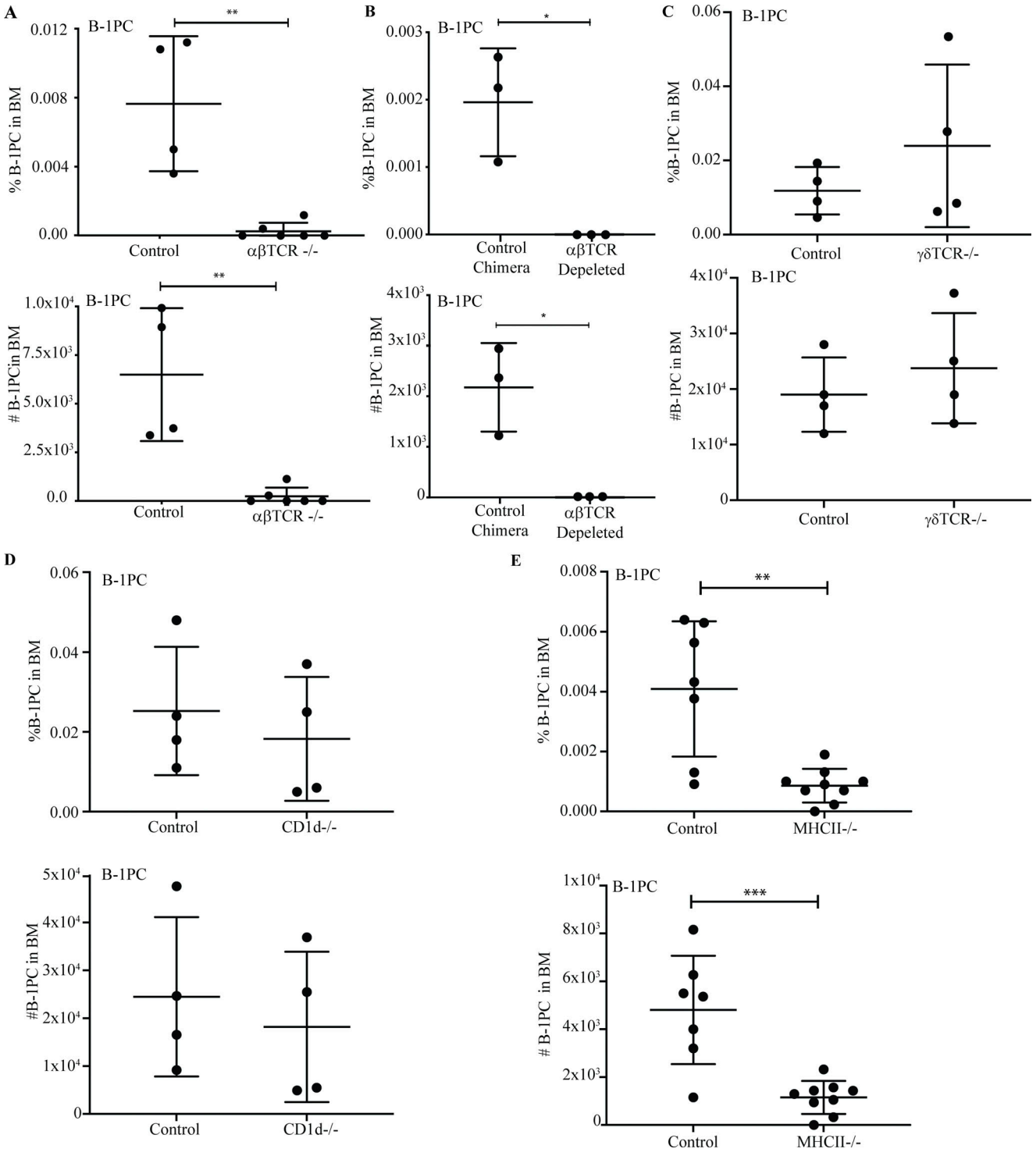

Figure 6. **BM B-1PC requires classical MHCII-restricted aβTCR CD4 T cell help. (A–E)** Mean percent ± SD live cells (top) and total number B-1PC in BM (bottom) of (A) C57BL/6 and aβTCR$^{-/-}$ mice (n = 4–6/group), (B) B cell allotype chimeric mice treated from birth with PBS (control) or with anti-βTCR mAb (H57-197; n = 3/group), (C) C57BL/6 and δTCR$^{-/-}$ mice (n = 4/group), (D) C57BL/6 and CD1d$^{-/-}$ mice (n = 4/group), and (E) C57BL/6 and MHCII$^{-/-}$ mice (n = 7–9/group). Values were compared by unpaired Student's t test. **, 0.001 ≤ P < 0.01; *, 0.01 ≤ P < 0.05.

antigen-binding CDR3 regions were dominated by a small number of distinct motifs (Fig. 10, C–E). Some of these motifs were present also among the CD5$^+$ and CD5$^-$ B-1 cells; however, they were enriched within the B-1PC compartment (Fig. 10 C). Furthermore, a number of these motifs were shared between individual mice, thus suggesting that the B-1PC compartment includes many "public" clones (Fig. 10 F). In addition, analysis of the nucleotide sequences of these CDR3 region motives revealed that they had minimal N-region alterations (Table S1) and were generated through the recombination of different *Ighv* and *Ighj*

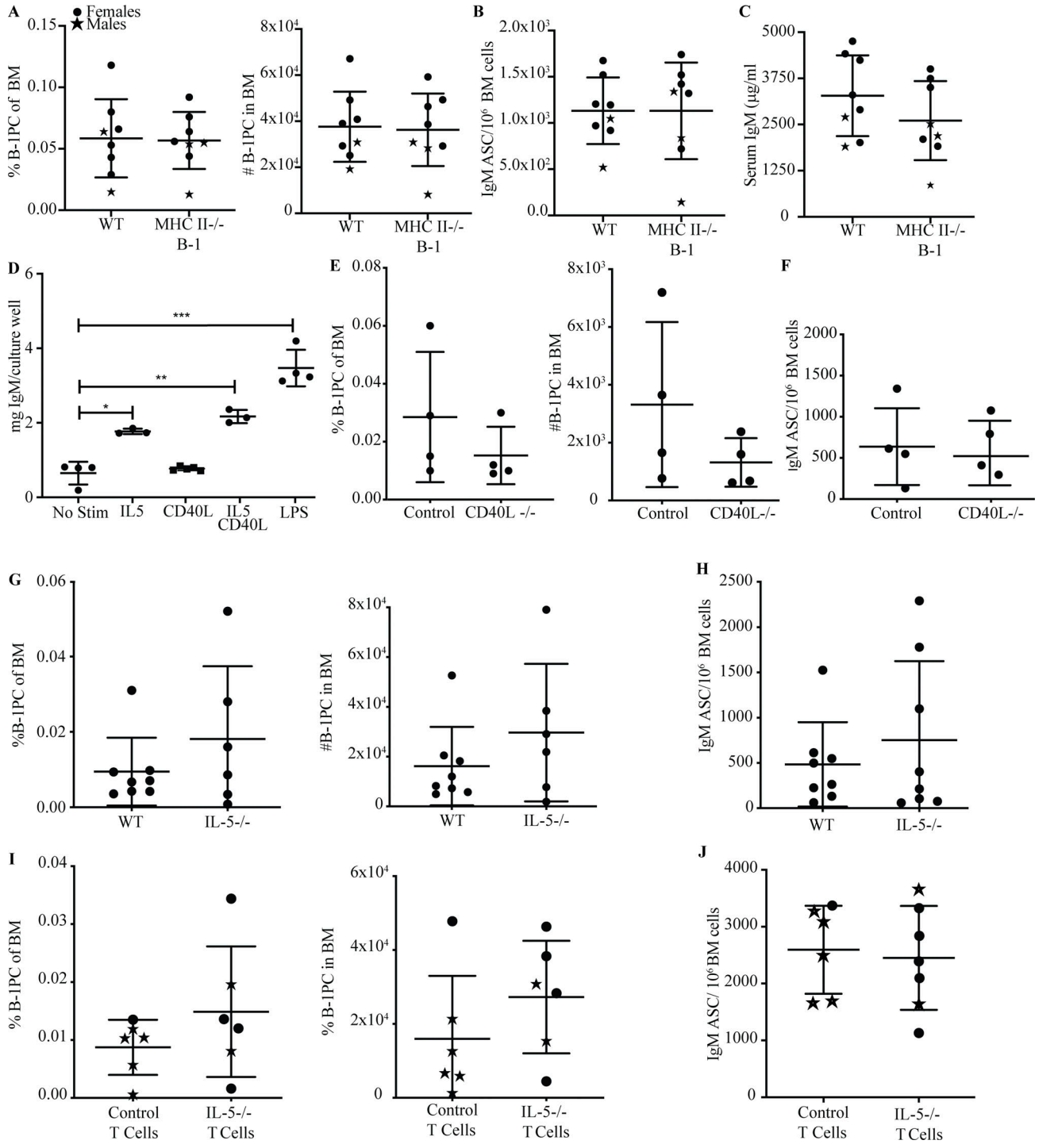

Figure 7. **T cell–dependent development of BM B-1 PC occurs in an MHCII, CD40L, and IL-5–independent manner. (A)** Mean percent ± SD live cells (left) and total number B-1PC (right) in BM of Rag1$^{-/-}$ mice reconstituted with C57BL/6 B-1 cells or MHCII$^{-/-}$ B-1 cells and C57BL/6 T cells. **(B)** Mean number ± SD BM IgM ASC per 10^6 total cells from mice in A (n = 8/group). **(C)** Mean ± SD serum IgM (µg/ml) from mice in A (n = 8/group). **(D)** IgM in culture supernatants of B-1 cells stimulated with IL-5, CD40L, or both (n = 3 culture wells/condition); includes no stim control and LPS-positive control. **(E)** Mean percent ± SD live cells (left) and total number B-1PC (right) in BM C57BL/6 mice and CD40L$^{-/-}$ mice (n = 4/group). **(F)** Mean number ± SD BM IgM ASC per 10^6 total cells from mice in E (n = 4/group). **(G)** Mean percent ± SD live cells (left) and total number B-1PC (right) in BM C57BL/6 mice and IL-5$^{-/-}$ mice (n = 8/group). **(H)** Mean number ± SD BM IgM ASC per 10^6 total cells from mice in G (n = 8/group). **(I)** Mean percent ± SD live cells (left) and total number B-1PC (right) in BM of Rag1$^{-/-}$ mice reconstituted with C57BL/6 B-1 cells and C57BL/6 T cells or IL-5$^{-/-}$ T cells. **(J)** Mean number ± SD BM IgM ASC per 10^6 total cells from mice in I (n = 8/group). Values in D were compared by one-way ANOVA with post hoc testing for multiple comparisons. ***, 0.0001 ≤ P < 0.001; **, 0.001 ≤ P < 0.01; *, 0.01 ≤ P < 0.05.

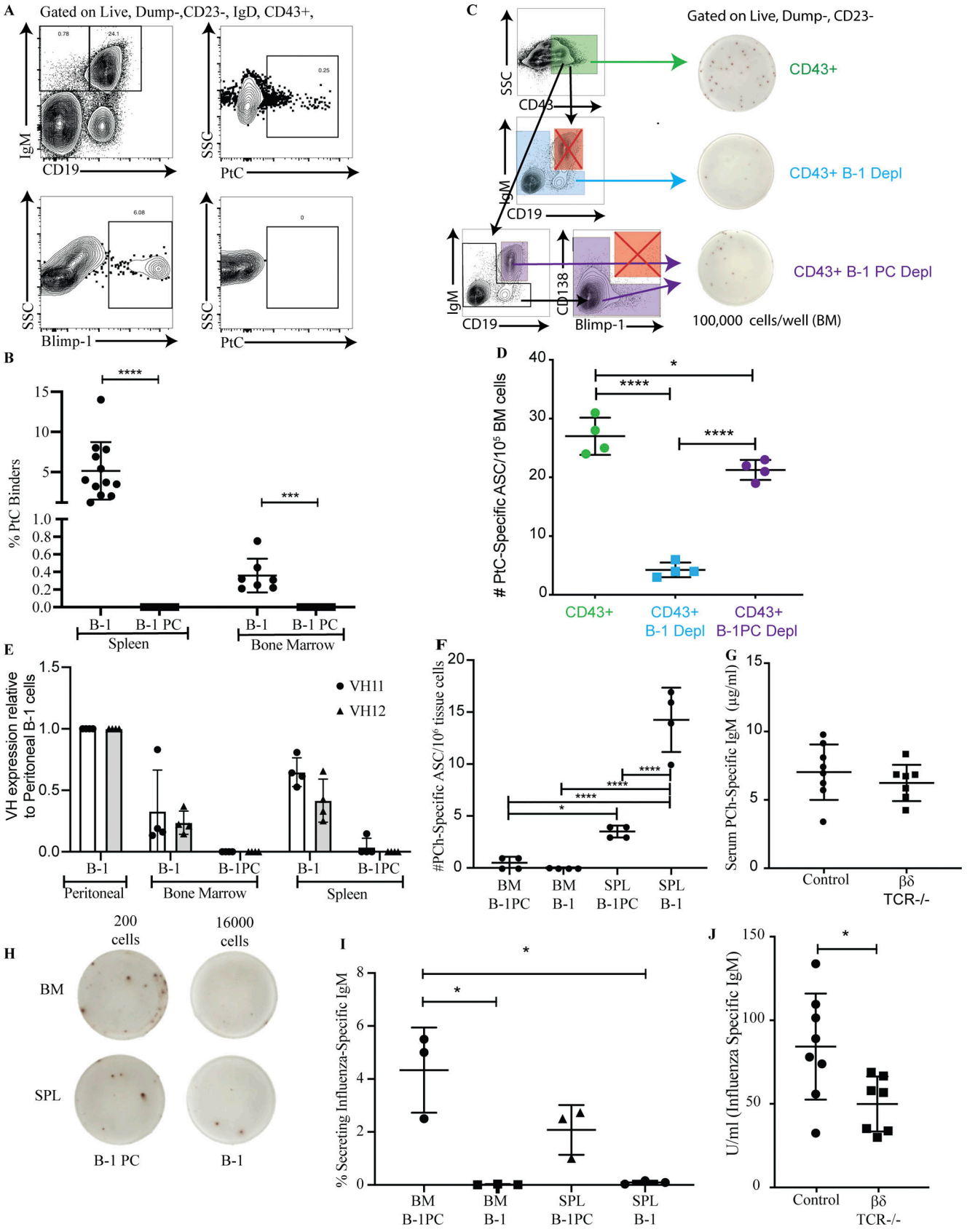

Figure 8. **B-1 and B-1 PC differ in antigen binding. (A)** Representative FACS plots of Blimp-YFP mice showing gating for B-1 and B-1PC binding fluorescently labeled PtC liposome. **(B)** Mean percent ± SD B-1 cells or B-1PC binding to PtC liposomes (n = 6–12 mice/group, a combination of three independent experiments). **(C)** Gating strategy for sorted populations of BM cells onto ELISPOT plates coated with PtC liposomes: CD43⁺ cells, CD43⁺ cells depleted of B-1 cells,

CD43+ cells depleted of B-1 PC, and corresponding representative ELISPOT wells. **(D)** Mean number ± SD of anti-PtC IgM ASC per 10^6 cells from populations defined in C (n = 4 replicates per group, combination of two independent experiments). **(E)** Relative expression of VH11 and VH12 BCR in BM and SPL B-1 populations as compared with peritoneal B-1 cells by FACS (n = 4 mice/group). **(F)** Mean number ± SD of anti-PCh IgM ASC from each population per 10^6 BM or spleen cells (n = 4 replicates per group, combination of two independent experiments). **(G)** Mean mg/ml ± SD of anti-PCh IgM in serum of control mice or mice lacking BM B-1 PC (TCR $\beta/\delta^{-/-}$ mice; n = 6–8 per group). **(H)** Representative ELISPOT of sorted B-1 and B-1PC from BM and spleen onto wells coated with influenza A/Puerto Rico/8/34. The number represents the total number of cells sorted into that well. **(I)** Mean percentage ± SD of cells in each population in G secreting anti-influenza IgM (n = 3 replicates per group). **(J)** Mean relative units ± SD of anti-influenza IgM in serum of control mice or mice lacking BM B-1 PC (TCR $\beta/\delta^{-/-}$ mice; n = 6–8 per group). Values were compared using a one-way ANOVA with post hoc Tukey or unpaired Student's t test where appropriate. *, $0.01 \le P < 0.05$; ***, $0.0001 \le P < 0.001$; ****, $P < 0.0001$.

genes, suggestive of stringent selection events favoring these motifs underlying their oligoclonality (Fig. 10 G). Thus, B-1PC generate a unique, highly selected, and public nIgM repertoire characterized by short junctional sequences, revealing new features of the secreted nIgM repertoire that are distinct from those previously associated with B-1 cells (Yang et al., 2015; Prohaska et al., 2018; Upadhye et al., 2019).

Discussion

It has been well documented that B-1 cells generate much of the circulating, broadly self-reactive nIgM in mice and that they do so seemingly independent of prior exposure to foreign antigens, including microbiota (Savage et al., 2017; Haury et al., 1997; Bos et al., 1989). The distinct developmental path of B-1 cells explains their unique capability of producing self-reactive nIgM. These cells arise mainly from fetal HSC and bypass the need for pre-BCR assembly and hence selection while requiring self-antigen reactivity for selection and/or expansion of immature B-1 into the mature B cell pool (Hayakawa et al., 1999; Wasserman et al., 1998; Wong et al., 2019; Hayakawa et al., 2003). The broad and seemingly polyreactive specificities of nIgM are reminiscent of pattern recognition receptors (PRRs), which recognize broad classes of foreign antigens/pathogens as well as "altered self" in the form of danger-associated molecular patterns (DAMPS). Like PRRs, the presence of nIgM is critical for the maintenance of both immune homeostasis and host defense (Baumgarth, 2011). Here, we identify the antigen-binding motives of the IgH-chains expressed by a major source of nIgM, BM B-1PC. The repertoire of B-1PC differs from that of B-1 cells sorted from the same tissues, as previously reported for B-1 cells from body cavities and spleen (Yang et al., 2015; Prohaska et al., 2018; Upadhye et al., 2019). Some of the repertoire's motifs expressed by B-1PCs have, however, been noted previously in BCR repertoire analyses conducted on total spleen cells (Rettig et al., 2018), further underscoring the abundance and presumably large contributions of these B-1PC to the nIgM pool.

The dominance of the B-1PC repertoire encoded by short Igh-CDR3 regions is distinct from the repertoire of previously identified, broadly neutralizing antibodies to HIV and influenza, which tend to be both highly mutated and contain very long CDR3 regions (Yu and Guan, 2014; Ekiert et al., 2012), suggesting distinct origins of these types of antibodies. Instead, the repertoire is reminiscent of that reported for B cells in human cord blood, which showed a preference for shorter CDR3 regions, and the presence of more public clones compared with B cells in adult blood (Guo et al., 2016). This provides a tangible link between nIgM generated by B-1PC in mice and fetal-derived B-1 cells in humans. While the presence of B-1 cells in humans has been controversial (Griffin et al., 2011), recent extensive comparative single-cell sequencing analysis of human fetal and adult tissues provided, to these authors, convincing evidence of human fetal origin "B-1" cells, which were seen only in human fetal but not adult-derived tissues (Suo et al., 2022). Interestingly, as described here for murine B-1PC, these cells were found to express shorter CDR3 regions than adult B cell counterparts taken from the same tissues (Suo et al., 2022). It is of course also further support for the abundance of evidence that has linked B-1 cell development to fetal developing precursors as the enzyme facilitating N-region editing, TdT, is not expressed until after birth (Feeney, 1990).

The development of the B-1PC–derived nIgM repertoire appears to be shaped by extensive selection and expansion resulting in the formation of a highly oligoclonal B-1PC pool, consistent with our findings that B-1PC development is delayed until a few weeks after birth. As expected from the PRR-like nIgM, the Igh-repertoire of B-1PC is broadly shared between individual mice, thus representing "public" clones. Their repertoire is restricted even further through convergent recombination, making it highly dominated by a handful of Igh-CDR3 region motifs.

Although the complete analysis of the B-1PC repertoire awaits single-cell sequencing of these rare cells and assessment of their light chains, the study demonstrates that the B-1 cell compartment provides at least two very distinct repertoires of nIgM, one generated by cells that terminally differentiate into B-1PC and the other by B-1_{sec}, the latter providing an estimated 25–30% of the circulating nIgM (Savage et al., 2017), but seemingly encoding much of what has been associated previously with B-1 cell–derived nIgM. BM B-1PC generated the presumably broadly reactive nIgM that can bind to influenza virus. This is a natural-occurring specificity that we have shown previously to be B-1 cell–derived and capable of suppressing viral replication early after virus infection and not requiring infection for its presence (Baumgarth et al., 1999, Baumgarth et al., 2000; Choi and Baumgarth, 2008; Waffarn et al., 2015). However, other previously identified specificities associated with B-1 cells, such as those to PCh or PtC-containing liposomes, were found to be generated by B-1_{sec} rather than B-1PC, even though both populations arise predominantly from fetal HSCs. B-1PC showed little expression of VH11 or VH12, did not bind to PtC-containing liposomes, and did not secrete anti-PtC or anti-PCh IgM, previously identified hallmarks of B-1 cells in spleen and body cavity (Carmack et al., 1990; Hardy et al., 1989; Conger et al., 1991; Briles et al., 1981).

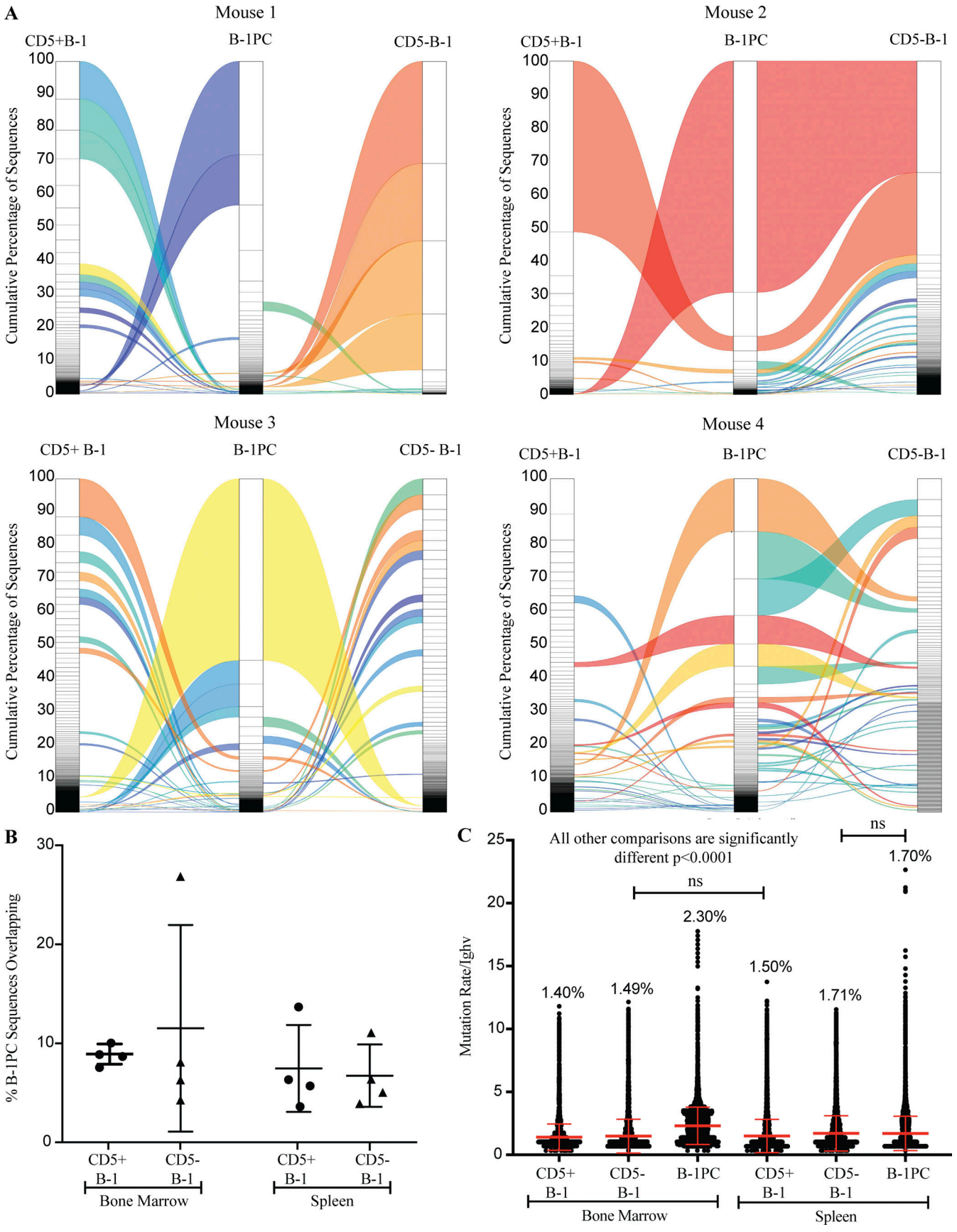

Figure 9. **B-1PC express a highly oligoclonal germline-encoded repertoire. (A)** Representative alluvial plots showing the cumulative number of sequences and overlap of CDR3 regions of B-1 cell subsets in BM. **(B)** Mean percent ± SD of overlapping sequences between B-1PC and CD5$^+$ or CD5$^-$ B-1 cells in both BM and spleen (n = 4 mice). **(C)** Mean number of mutations ± SD of Ighv sequences recovered from identified cell populations.

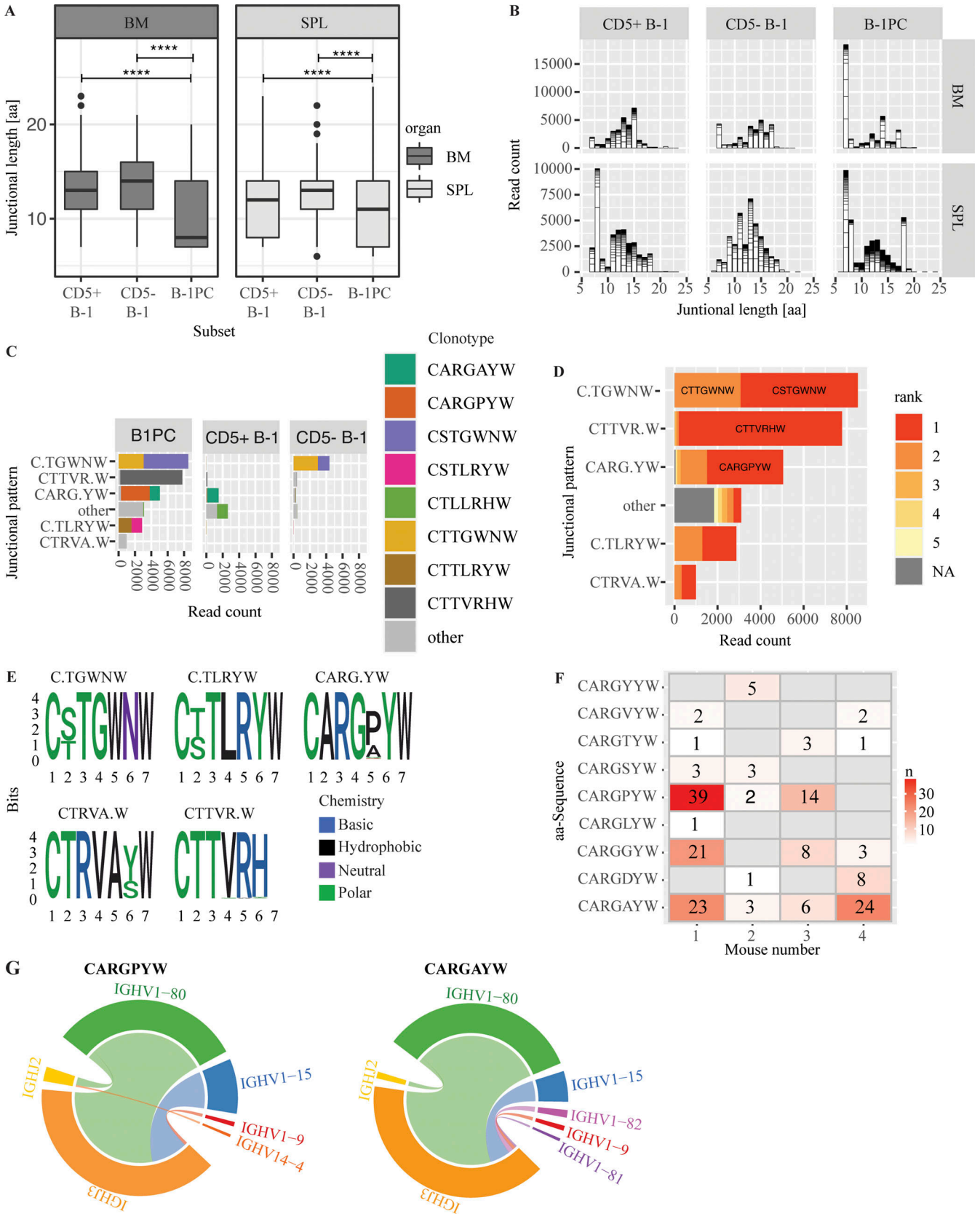

Figure 10. **B-1PC express a unique, public repertoire with short junctional sequences. (A)** Mean junctional lengths among indicated B cell subsets in BM and spleen. **(B)** Distribution of junctional lengths by read count in indicated B cell subsets from BM (top) and spleen (bottom). **(C)** Distribution of 7 amino acid junctional sequences in B cell subsets. **(D)** Rank by read count of 7 amino acid junctional sequences in B-1PC. **(E)** Position weight matrix for the five most abundant junctional patterns. **(F)** Nine distinct clonotypes encode the abundant "CARG.YW" motif, one indicated per row, and their distribution among the four

individual mice studied (columns) reveals many shared public clones. Numbers identify unique occurrences. **(G)** Depiction of different combinations of V and J genes that encode two identical shared sequences, suggestive of convergent recombination.

The abundance of PtC-binding and VH11/VH11-expressing peritoneal cavity B-1 cells (Conger et al., 1991; Carmack et al., 1990; Hardy et al., 1989; Yang et al., 2015; Prohaska et al., 2018) and their absence among B-1PC suggests that most PtC-binding B-1 cells require signals distinct from those causing B-1PC differentiation into nIgM-ASC and differentiate into B-1_{sec}. In support, we demonstrate here that BM B-1PC, but not B-1_{sec}, require the presence of CD4 T cells for differentiation. With regards to the PtC-binding body cavity CD5$^+$ B-1 cells, it is also noteworthy that previous studies suggested them to be less likely to differentiate into IgM ASC compared with non-PtC-binding CD5$^+$ B-1 cells (Wang et al., 2012). This could thus also suggest that PtC-binding B-1 cells fulfill functions that are distinct from those and/or in addition to those involving IgM secretion.

Innate activation leads to the differentiation of body cavity B-1 cells into IgM ASC in vitro as well as in vivo, where these signals drive CD5$^+$ B-1 cells from the body cavity into secondary lymphoid tissues prior to their differentiation (Waffarn et al., 2015; Savage et al., 2019; Kawahara et al., 2003). While this could suggest a precursor–product relationship between the non-secreting body cavity B-1 cells and the nIgM-secreting B-1 cells in spleen and BM, these events represent responses to changes to immune homeostasis and may not reflect the mechanisms by which steady-state nIgM secretion is induced and/or regulated.

T cell dependence of BM B-1PC differentiation was unexpected given that depletion of T cells or T cell deficiency has not been reported previously to cause obvious reductions in serum IgM concentrations (Madsen et al., 1999; Hooijkaas et al., 1985; Van Oudenaren et al., 1984). Our data provide an explanation for this apparent discrepancy by demonstrating that only the development of BM B-1PC but not spleen B-1PC or B-1_{sec} required CD4 T cells. In addition, making up for the lack of BM B-1PC in the absence of CD4 T cells was the expansion in the number of BM B-1_{sec}, which seem to reconstitute, at least in magnitude, nIgM production. However, nIgM to influenza in T-deficient mice remained at serum concentrations lower than those in wild-type controls, further supporting the differences in the repertoire of nIgM produced by B-1PC and B-1_{sec}. The compensatory increases in B-1_{sec} differentiation appear restricted to a subset of fetal/neonatal-derived B-1 cells, however, as body cavity–derived B-1 cells from adult mice did not differentiate into B-1_{sec} following their adoptive transfer, even when transferred into a neonatal environment. The latter is consistent with two previous studies that had noted reduced nIgM levels in mice reconstituted with adult B-1 cells when transferred into an adult T cell–deficient environment (Moon et al., 2004; Reynolds et al., 2015). This is significant as it suggests different functionalities between B-1 cells arising from various waves of fetal and neonatal development and also suggests the loss of certain B-1 cell types as mice age (Montecino-Rodriguez and Dorshkind, 2012; Holodick and Rothstein, 2015; Holodick et al., 2016).

The exact nature of the help being provided for BM B-1PC development by TCRαβ$^+$ CD4$^+$ MHC class II–restricted T cells remains to be more fully explored. It required classical TCRα/β MHCII-restricted CD4 T cells, but not B cell expression of MHCII and CD40, or IL-5 production by T cells. CD4 T cell–mediated help appeared needed for the differentiation but not maintenance of BM B-1PC, as depletion of CD4 T cells in adulthood had no effect on BM B-1PC numbers or serum IgM levels. Given that spleen B-1PC development does not require T cell help and thus B-1PC differentiation per se can occur without T cells, it remains possible that BM B-1PC reside in a particular BM niche that requires CD4 T cells for its development, but once established, is maintained without T cells.

Alternatively, signals provided by CD4 T cells directly to B-1 cells allow their differentiation into BM B-1PC. Although B-1 cells express relatively high levels of CD86 and were shown previously to activate T cells in both, an antigen-specific and non-specific manner (Hsu et al., 2014; Margry et al., 2013; Zimecki and Kapp, 1994; Zimecki et al., 1994), very little is known about what impact these interactions have on B-1 cells. NKT cells and TH17 cells have been implicated in activation of B-1 cells during active infection or inflammation (Jackson-Jones et al., 2016; Wang et al., 2016; Campos et al., 2006)., but as we show here, depletion of CD1 does not affect BM B-1PC, and IL-17 is unlikely responsible for regulating steady-state nIgM production. T cell–derived IL-5 can promote PCh-specific nIgM (McKay et al., 2017), but anti-PCh nIgM does not appear to come from BM, but rather from spleen B-1PC and B-1_{sec}. Furthermore, although IL-5R deficiency has been shown to reduce serum IgM levels, it did so in a T-independent manner (Moon et al., 2004), and more recent studies have shown ILCs to be a source for IL-5–mediated B-1 cell activation (Jackson-Jones et al., 2016; Barbosa et al., 2021).

In summary, our data demonstrate the presence of multiple distinct differentiation pathways that shape the pool of nIgM. The hallmarks of nIgM generated by B-1PC are their short CDR3 regions and the presence of but a handful of distinct Igh-CDR3 region motifs, not previously associated with B-1 cells. This leaves specificities such as phospholipids, PCh and PtC previously associated with B-1 cells (Arnold and Haughton, 1992; Conger et al., 1991; Briles et al., 1981) to the small pool of non-terminally differentiated B-1_{sec}, whose development appears restricted in ontogeny.

Materials and methods

Mice

7- to 8-wk-old male and female C57BL/6J (control), B6.129S6-Del(3Cd1d2-Cd1d1)1Sbp/J (CD1d$^{-/-}$), B6.129P2-*Tcrβ*^{tm1Mom}/J (TCRβ$^{-/-}$) and B6.129P2-*Tcrd*^{tm1Mom}/J (TCRδ$^{-/-}$) mice and breeding pairs of C57BL/6J, B6.129S2-H2$^{dlAb1\text{-}Ea}$/J (MHCII$^{-/-}$), B6.129P2-*Tcrb*^{tm1Mom} *Tcrd*^{tm1Mom}/J (TCRβδ$^{-/-}$), B6.129S7-*Rag1*^{tm1Mom}/J (Rag-1$^{-/-}$), B6.Cg-Gpi1^a Thy1^a Igh^a/J

(Igha), C57BL/6-Il5^{tm1Kopf}/J (IL-5$^{-/-}$), and B6.129S-*Cd40lg*^{tm1Imx}/J (CD40L$^{-/-}$) were purchased from The Jackson Laboratory. 6-wk-old male and female SPF Swiss Webster mice were ordered from Taconic. Breeding pairs of B6.Cg-Tg(Prdm1-EYFP) 1Mnz/J (Blimp-1 YFP) were generously provided by Michel Nussenzweig (The Rockefeller University, New York, NY, USA). Germ-free Swiss Webster mice, age- and sex-matched to the SPF controls, were generously maintained and provided by Andreas Bäumler (University of California, Davis [UC Davis], Davis, CA, USA).

Neonatal chimeras were generated as described previously (Baumgarth et al., 1999). Briefly, neonatal Igha mice were treated twice weekly with intraperitoneal injections of DS-1.1 (anti-IgMa) in PBS, beginning on day one after birth for a total of 2.3 mg over 42 d to deplete B cells. Between days 2–4, mice were given 5 × 10^6 non-sorted donor cells from the peritoneal cavity washout of C57BL/6J (IgMb) mice as a source of B-1 cells. Mice were rested for at least 42 d after last anti-IgM injection before use in experiments to allow for donor B-2 cell reconstitution. CD4 and TCRβ depletion was performed by i.p. injection of 0.5 mg/mouse of anti CD4 mAb (GK1.5) or anti-TCRβ mAb (H57.197) on day 1 of depletion followed by 0.3 mg/mouse twice weekly for the duration of the experiment.

Reconstituted neonatal Rag-1$^{-/-}$ mice were generated by intraperitoneal injection of 1 × 10^6 MACS enriched (>94% purity) peritoneal B-1 cells +/− 1 × 10^6 splenic CD4$^+$ T cells (purity above 95%) at 3–6 d of age. They were kept for at least 12 wk before use. Reconstituted adult Rag-1$^{-/-}$ mice were generated by intraperitoneal injection of FACS-sorted (>98% purity) ∼5 × 10^5 peritoneal B-1 cells only, ∼5 × 10^5 peritoneal B-1 cells + ∼5 × 10^5 splenic CD4$^+$ T cells (>99% purity), or ∼5 × 10^5 peritoneal cells depleted of B-1 cells at 6–8 wk of age. They were allowed to reconstitute for 7 wk. Mice were used between 8 and 14 wk of age for Blimp-1YFP, Swiss Webster, TCRβδ$^{-/-}$, TCRβ$^{-/-}$ TCRδ$^{-/-}$, CD1d$^{-/-}$, MHCII$^{-/-}$, and control (B6, Igha) mice, between 12 wk and 6 mo of age for neonatal chimeras and between 12 and 16 wk of age for reconstituted neonatal Rag-1$^{-/-}$ mice. All mice used for experiments were female unless otherwise indicated. All mice were maintained in microisolator cages under SPF conditions, were provided mouse chow and water supplied at lib by the UC Davis Animal Care staff, and were euthanized by overexposure to CO_2. All procedures were approved by the UC Davis Institutional Animal Care and Use Committee.

B-1 cell magnetic cell separation

Single-cell suspensions of peritoneal cavity washout and spleen cells were counted and blocked with anti-FcR (2.4.G2). For B-1 cell enrichment, peritoneal cavity cells were labeled with biotinylated anti-F4/80 (F4/80), Gr1 (RA3.6C2), NK1.1 (DX5), CD4 (GK1.5), CD8a (53–6.7.3.1), CD23 (B3B4), and CD90.2 (30H12.1) generated in-house and splenic CD4 T cells were enriched by labeling with biotinylated anti-F4/80, Gr-1, CD8a, TCRδ (GL-3), NK1.1, CD19 (ID3), and CD11b (MAC1.13) followed by staining with anti-biotin magnetic beads (Miltenyi Biotec) and passing over a magnetic column (auto-MACS, Miltenyi Biotec). Purity for peritoneal B-1 cells was >94% and purity for splenic CD4 T cells was ≥95%.

Generation of lineage tracing FlkSwitch chimeras

Recipient C57BL/6 mice (8–12 wk) were either sublethally (750 cGy) or lethally irradiated (1,000 cGy, split dose) using a Precision X-Rad 320. Transplantations were performed by FACS-sorting GFP$^+$ drHSC, only present during fetal and neonatal development, and Tom$^+$ HSC (CD150$^+$ cKit$^+$ Sca1$^+$ Lin$^-$) from the fetal liver of FlkSwitch mice (Beaudin et al., 2016; Boyer et al., 2011). 200 sorted GFP$^+$ drHSC or Tom$^+$ HSC in 100–200 µl were transferred via retroorbital injection with (for lethally irradiated mice) or without 5 × 10^6 whole BM cells from C57BL/6 mice. At 18 wk, recipients were euthanized and cell populations were assessed for chimerism by flow cytometry. Long-term multilineage reconstitution was defined as >1% chimerism in all mature blood lineages.

Flow cytometry and FACS sorting

BM and spleen were processed as previously described (Rothaeusler and Baumgarth, 2006). All buffers used for staining were azide free. Briefly, BM was harvested by injecting staining media through the marrow cavity of a long bone, and a single-cell suspension was made by pipette agitation and filtering through a 70-µm nylon mesh. A single-cell suspension of the spleen was made by grinding the tissue between the frosted ends of two microscope slides and filtered through a 70-µm nylon mesh. All samples were then treated with ACK lysis buffer (Rothaeusler and Baumgarth, 2006), refiltered through nylon mesh, and suspended in staining media. Peritoneal/pleural cavity cells were obtained using staining media flushed into and then aspirated from the peritoneal and pleural cavities with a glass pipette and bulb or a plastic pipette (Molecular Bio Products, Inc.). Trypan Blue exclusion dye was performed on all samples to identify live cells using a hemocytometer or an automated cell counter (Nexcelom Bioscience). Cells were blocked with anti-FcR (2.4.G2), washed, and stained with fluorescent antibodies (Table S2).

PtC-containing liposomes were generously provided by Aaron Kantor (Stanford University, Stanford, CA, USA). Dead cells were identified using Live/Dead Fixable Aqua or Live/Dead Fixable Violet stain (Invitrogen). Fluorescently labeled cells were read on either a four-laser, 22-parameter LSR Fortessa (BD Bioscience), or a five-laser, 30-parameter Symphony (BD Bioscience). FACS-sorting was done using a three-laser FACSAria (BD Bioscience) equipped with a 100-µm nozzle at low pressure to avoid PC death. Data were analyzed using FlowJo software (FlowJo LLC, kind gift of Adam Treister, Gladstone Institute, San Francisco, CA). Peritoneal B-1 cells are identified as Dump$^-$ (CD4, CD8a, Nk1.1, F4/80, Gr-1), CD23$^-$, and CD19^{hi}. Splenic CD4$^+$ T cells were identified as Dump$^-$ (CD19, CD8a, NK1.1, F4/80, Gr-1, TCRγδ, CD138), CD3$^+$, and CD4$^+$. BM and spleen B-1 cells are identified as Dump$^-$, CD23$^-$ C43$^+$, IgD$^-$, IgM$^+$, and CD19^{hi}; and B-1PC are identified as Dump$^-$, CD23$^-$ C43$^+$, IgD$^-$, IgM$^+$, CD19$^{lo/-}$ and Blimp-1; and/or CD138$^+$. FACSAria-sorted cells for adoptive transfer had a purity of >98% for peritoneal B-1 cells and peritoneal cells depleted of B-1 cells and ≥99% for splenic CD4 T cells.

ELISPOT

IgM antibody ASC were enumerated as described previously (Doucett et al., 2005). Briefly, 96-well ELISPOT plates (MultiScreen HA Filtration, Millipore) were coated with 5 µg/ml anti-IgM (331), whole killed influenza PR8/34 A (400 HAU/ml; in house), Phosphorylcholine-BSA (Biosearch Technologies; 0.625 µg/ml), or 110 nm 1,2-dioleoyl-sn-glycero-3-phosphocholine liposomes (FormuMax, 10 mg/ml in 100% ethanol). Non-specific binding was blocked with 4% BSA in PBS. Tissues were processed as detailed above and cells were plated in culture media (RPMI 1640, 10% fetal bovine serum, 292 µg/ml *L*-glutamine, 100 U/ml penicillin, 100 µg/ml streptomycin, and 50 µM 2-mercaptoethanol). Cells were twofold serially diluted and cultured overnight (~16 h) at 37°C/5% CO_2. Deionized water was used to lyse the cells after which IgM secretion was revealed with biotinylated anti-IgM (Southern Biotech), followed by streptavadin-horseradish peroxidase (Vector Labs), both diluted in 2% BSA in PBS. Last, a substrate solution (3.3 mg 3-amino-9-ethylcarbazole [Sigma-Aldrich] dissolved in dimethyl formamide and 0.015% hydrogen perioxide in 0.1 M sodium acetate was added and the reaction was stopped with deionized water. Spots were enumerated and images were captured with the AID EliSpot Reader System (Autoimmun Diagnostika).

ELISA

Sandwich ELISA was performed as previously described (Rothaeusler and Baumgarth, 2006). ELISA plates (MaxiSorp 96-well plates, Thermo Fisher) were coated with unlabeled anti-IgM (Southern Biotech or mAb 331), whole killed influenza PR8/34 A (400 HAU/ml; in house), phosphorylcholine-BSA (Biosearch Technologies; 0.625 µg/ml), or 110 nm 1,2-dioleoyl-sn-glycero-3-phosphocholine liposomes (FormuMax; 10 mg/ml in 100% ethanol). Non-specific binding was blocked with 1% newborn calf serum, 0.1% dried milk powder, and 0.05% Tween 20 in PBS (ELISA blocking buffer). Serum and standards were added to the plate at previously determined predilutions and were twofold serially diluted. Binding was revealed with biotinylated anti-IgM (Southern Biotech), anti-IgMa (BD Bioscience), or anti-IgMb (BD Bioscience), and then streptavadin-horseradish peroxidase (Vector Labs), all diluted in ELISA blocking buffer and substrate (0.005% 3,3′,5,5′-tetramethylbenzidine in 0.05 M citric acid buffer and 0.015% hydrogen peroxide). The reaction was stopped with 1 N sulfuric acid. Absorbance was measured at 450 nm (595 nm reference wavelength) on a spectrophotometer (SpectraMax M5, Molecular Devices). IgM concentrations in the samples were determined by comparison to curves generated by the isotype standards or hyperimmune serum (influenza). The PCh standard was a kind gift from Karen Haas (Wake Forest University, Winston-Salem, NC, USA).

Autoantigen array

10 µl of serum from TCRβ/δ$^{-/-}$, CD4^{+}-depleted Ig-allotype chimeras, and B-1 cell–reconstituted Rag1$^{-/-}$ mice, as well as their T cell–sufficient controls, were treated with DNAse1, diluted 1:50, and incubated with the autoantigen array chip. IgM binding to the autoantigens was detected with Cy5-labeled anti-IgM, and the chips were read using GenePix 4400A Microarray Scanner (Molecular Devices). The images were analyzed using GenePix7.0 software (Molecular Devices). The average net fluorescent intensity of each autoantigen was normalized to an internal IgM control.

In vitro B-1 cell cultures

autoMACS-enriched B-1 cells were cultured at 1 × 10^{5} cells/well in 96-well round bottom plates with no stimulation (negative control), IL-5 (8 ng/ml), CD40L (60 ng/ml), IL-5 and CD40L, or LPS (10 µg/ml; positive control) for 72 h at 37°C. Supernatants were then collected for IgM ELISA.

BCR sequencing and repertoire analysis

3,000 cells of the following populations from Blimp-1 YFP reporter mice were FACS-sorted into RLT buffer (Qiagen) using FACSAria: BM CD5^{+} B-1 (Dump^{-}, CD23^{-} C43^{+}, IgD^{-}, IgM^{+}, CD19^{hi}, CD5^{+}), BM CD5^{-} B-1 (Dump^{-}, CD23^{-} C43^{+}, IgD^{-}, IgM^{+}, CD19^{hi}, CD5^{-}), and BM B-1PC (Dump^{-}, CD23^{-} C43^{+}, IgD^{-}, IgM^{+}, CD19$^{lo/-}$, and Blimp-1 YFP^{+}). Total cellular RNA was extracted using the RNeasy Mini kit by following the manufacturer's protocol (Qiagen). Approximately 20 ng of RNA was used for reverse transcription using the iScript cDNA synthesis kit (BioRad). Mouse IGH V gene transcripts were amplified by two rounds of nested PCR starting from 2.5 µl of cDNA as a template using the primers in Table S3. Inner primers were appended to Illumina Nextera sequencing tags (F tag: 5′-TCG TCGGCAGCGTCAGATGTGTATAAGAGACAG-3′; R tag: 5′-GTCTCG TGGGCTCGGAGATGTGTATAAGAGACAG-3′).

All PCR reactions were performed in 96-well plates in a total volume of 25 µl containing 200 nM of each primer. In brief, 200 nM of 5′ oligo and an equimolar mixture of 3′ oligos (final concentration 200 nM) were used for nested PCRs (Table S3) using High-Fidelity Platinum PCR Supermix (Invitrogen). Nested PCR1 was performed as follows: denaturation at 94°C for 15 min followed by 50 cycles of 94°C for 30 s, 60°C for 30 s, 72°C for 55 s, and final incubation at 72°C for 10 min. Nested PCR2 was performed using 0.5 µl of unpurified first-round PCR product as the template. Conditions were as follows: 94°C for 15 min followed by 50 cycles of 94°C for 30 s, 68°C for 30 s, 72°C for 45 s, and final incubation at 72°C for 10 min.

Nextera (Illumina) indices were added via PCR described earlier (Tipton et al., 2015). Final purified PCR products were analyzed, pooled, and denatured before running on a MiSeq (Illumina) using the 300 bp × 2 v3 kit with a depth of ~500,000 sequences per sample.

Sequences were quality filtered using length thresholds of 200–600 bp and sequences with more than 15 bp less than Q30, more than 5 bp less than Q20, and any bp less than Q10 were eliminated. Sequences were aligned with IMGT/HighVquest (Alamyar et al., 2012) and were then analyzed for V region mutations and clonality using programs developed in-house and made previously available for public use. All clonal assignments were based on matching V and J regions, matching CDR3 length, and 85% CDR3 homology. Matlab or R scripts were used for visualization (Tipton et al., 2015). BCR sequences are deposited in the Sequence Read Archive under accession no. PRJNA781755.

Quantification and statistical analysis

All statistics were done with the help of Prism software (GraphPad Software) or the R software version 4.0.3 (R Core Team, 2020) with packages ggseqlogo (Wagih, 2017) and circlize (Gu et al., 2014).

Comparisons between the two groups were done using a two-tailed Student's *t* test. For more than two groups, a one-way ANOVA was performed with post hoc analysis for significant differences between individual groups using Tukey's correction for multiple comparisons. Time courses were analyzed using a two-way ANOVA with post hoc analysis for differences between conditions at each time point and between different timepoints in the same condition using a Šidák correction for multiple comparisons. Correlation analysis was done using Pearson's test, and a simple linear regression was performed to identify a best-fit line and 95% confidence interval. A $P < 0.05$ was considered statistically significant.

Online supplemental material

The supplemental material includes large comprehensive heatmaps of the autoantigen array data (Fig. S1) and the BCR repertoire analysis (Fig. S2), a list of repertoire sequences showing N-region insertions (Table S1), and two tables referred to in the Materials and methods section that list the antibody conjugates utilized for flow cytometry (Table S2) and the primer sequences used for BCR sequencing (Table S3).

Acknowledgments

The authors would like to thank Tracey Rourke for expert help with flow cytometry, and Dr. Chengsong Zhu (University of Texas Southwestern, School of Medicine) for autoantibody analysis. We also thank Drs. Karen Hass (Wake Forest School of Medicine, Winston-Salem, NC, USA) for an anti-PCh IgM standard, Gregg Silverman (New York University, School of Medicine, New York, NY, USA) for anti-PCh and anti-PtC IgM standards, and Dr. Aaron Kantor (Stanford University School of Medicine, Stanford, CA, USA) for PtC liposomes.

This work was supported by National Institutes of Health/National Institutes of Allergy and Infectious Diseases grants R01AI117890, R01AI148652, and R21AI151995 (to N. Baumgarth), T32 OD011147 (to F.L. Smith), R01AI121252, P01AI125180, and U01AI141993 (to F.E.-H. Lee); National Institutes of Health/National Heart, Lung, and Blood Institute grants R01HL147081 and K01 HL130753, as well as the Pew Biomedical Scholars Award and Hellman Fellow Award (to A.E. Beaudin); and The Research Council of Norway grant 268085 UiT and a travel grant from The Arctic University of Norway (to I. Jensen).

Author contributions: Conceptualization: N. Baumgarth, F.L. Smith, H.P. Savage, and S. Keller. Methodology: F.L. Smith, N. Baumgarth, H.P. Savage, S. Keller, Z. Luo, C.M. Tipton, A.C. Apostol, A.E. Beaudin, D.A. Lopez, and I. Jensen. Investigation: F.L. Smith, H.P. Savage, Z. Luo, C.M. Tipton, I. Jensen, and S. Keller. Visualization: F.L. Smith, H.P. Savage, N. Baumgarth, A.C. Apostol, C.M. Tipton, and S. Keller, Funding acquisition: N. Baumgarth, A.E. Beaudin, and F.E.-H. Lee. Project administration: N. Baumgarth. Supervision: N. Baumgarth, A.E. Beaudin, and FEL. Writing—original draft: F.L. Smith and N. Baumgarth. Writing—review & editing: N. Baumgarth, F.L. Smith, H.P. Savage, C.M. Tipton, F.E.-H. Lee, A.E. Beaudin, I. Jensen, and S. Keller.

Disclosures: The authors declare no competing interests exist.

Submitted: 2 February 2022
Revised: 1 August 2022
Accepted: 27 January 2023

References

Alamyar, E., P. Duroux, M.P. Lefranc, and V. Giudicelli. 2012. IMGT(®) tools for the nucleotide analysis of immunoglobulin (IG) and T cell receptor (TR) V-(D)-J repertoires, polymorphisms, and IG mutations: IMGT/V-QUEST and IMGT/HighV-QUEST for NGS. *Methods Mol. Biol.* 882: 569–604. https://doi.org/10.1007/978-1-61779-842-9_32

Alugupalli, K.R., and R.M. Gerstein. 2005. Divide and conquer: Division of labor by B-1 B cells. *Immunity*. 23:1–2. https://doi.org/10.1016/j.immuni.2005.07.001

Alugupalli, K.R., R.M. Gerstein, J. Chen, E. Szomolanyi-Tsuda, R.T. Woodland, and J.M. Leong. 2003. The resolution of relapsing fever borreliosis requires IgM and is concurrent with expansion of B1b lymphocytes. *J. Immunol.* 170:3819–3827. https://doi.org/10.4049/jimmunol.170.7.3819

Arnold, L.W., and G. Haughton. 1992. Autoantibodies to phosphatidylcholine. The murine antibromelain RBC response. *Ann. N. Y. Acad. Sci.* 651: 354–359. https://doi.org/10.1111/j.1749-6632.1992.tb24635.x

Atif, S.M., S.L. Gibbings, E.F. Redente, F.A. Camp, R.M. Torres, R.M. Kedl, P.M. Henson, and C.V. Jakubzick. 2018. Immune surveillance by natural IgM is required for early neoantigen recognition and initiation of adaptive immunity. *Am. J. Respir. Cell Mol. Biol.* 59:580–591. https://doi.org/10.1165/rcmb.2018-0159OC

Barbosa, C.H.D., L. Lantier, J. Reynolds, J. Wang, and F. Re. 2021. Critical role of IL-25-ILC2-IL-5 axis in the production of anti-Francisella LPS IgM by B1 B cells. *PLoS Pathog.* 17:e1009905. https://doi.org/10.1371/journal.ppat.1009905

Baumgarth, N. 2011. The double life of a B-1 cell: Self-reactivity selects for protective effector functions. *Nat. Rev. Immunol.* 11:34–46. https://doi.org/10.1038/nri2901

Baumgarth, N., O.C. Herman, G.C. Jager, L. Brown, L.A. Herzenberg, and L.A. Herzenberg. 1999. Innate and acquired humoral immunities to influenza virus are mediated by distinct arms of the immune system. *Proc. Natl. Acad. Sci. USA*. 96:2250–2255. https://doi.org/10.1073/pnas.96.5.2250

Baumgarth, N., O.C. Herman, G.C. Jager, L.E. Brown, L.A. Herzenberg, and J. Chen. 2000. B-1 and B-2 cell-derived immunoglobulin M antibodies are nonredundant components of the protective response to influenza virus infection. *J. Exp. Med.* 192:271–280. https://doi.org/10.1084/jem.192.2.271

Beaudin, A.E., S.W. Boyer, J. Perez-Cunningham, G.E. Hernandez, S.C. Derderian, C. Jujjavarapu, E. Aaserude, T. MacKenzie, and E.C. Forsberg. 2016. A transient developmental hematopoietic stem cell gives rise to innate-like B and T cells. *Cell Stem Cell*. 19:768–783. https://doi.org/10.1016/j.stem.2016.08.013

Boes, M., C. Esau, M.B. Fischer, T. Schmidt, M. Carroll, and J. Chen. 1998. Enhanced B-1 cell development, but impaired IgG antibody responses in mice deficient in secreted IgM. *J. Immunol.* 160:4776–4787. https://doi.org/10.4049/jimmunol.160.10.4776

Boes, M., T. Schmidt, K. Linkemann, B.C. Beaudette, A. Marshak-Rothstein, and J. Chen. 2000. Accelerated development of IgG autoantibodies and autoimmune disease in the absence of secreted IgM. *Proc. Natl. Acad. Sci. USA*. 97:1184–1189. https://doi.org/10.1073/pnas.97.3.1184

Bohannon, C., R. Powers, L. Satyabhama, A. Cui, C. Tipton, M. Michaeli, I. Skountzou, R.S. Mittler, S.H. Kleinstein, R. Mehr, et al. 2016. Long-lived antigen-induced IgM plasma cells demonstrate somatic mutations and contribute to long-term protection. *Nat. Commun.* 7:1–13. https://doi.org/10.1038/ncomms11826

Bos, N.A., H. Kimura, C.G. Meeuwsen, H. De Visser, M.P. Hazenberg, B.S. Wostmann, J.R. Pleasants, R. Benner, and D.M. Marcus. 1989. Serum immunoglobulin levels and naturally occurring antibodies against

carbohydrate antigens in germ-free BALB/c mice fed chemically defined ultrafiltered diet. *Eur. J. Immunol.* 19:2335–2339. https://doi.org/10.1002/eji.1830191223

Boyer, S.W., A.E. Beaudin, and E.C. Forsberg. 2012. Mapping differentiation pathways from hematopoietic stem cells using Flk2/Flt3 lineage tracing. *Cell Cycle*. 11:3180–3188. https://doi.org/10.4161/cc.21279

Boyer, S.W., A.V. Schroeder, S. Smith-Berdan, and E.C. Forsberg. 2011. All hematopoietic cells develop from hematopoietic stem cells through Flk2/Flt3-positive progenitor cells. *Cell Stem Cell*. 9:64–73. https://doi.org/10.1016/j.stem.2011.04.021

Briles, D.E., M. Nahm, K. Schroer, J. Davie, P. Baker, J. Kearney, and R. Barletta. 1981. Antiphosphocholine antibodies found in normal mouse serum are protective against intravenous infection with type 3 streptococcus pneumoniae. *J. Exp. Med.* 153:694–705. https://doi.org/10.1084/jem.153.3.694

Campos, R.A., M. Szczepanik, M. Lisbonne, A. Itakura, M. Leite-de-Moraes, and P.W. Askenase. 2006. Invariant NKT cells rapidly activated via immunization with diverse contact antigens collaborate in vitro with B-1 cells to initiate contact sensitivity. *J. Immunol.* 177:3686–3694. https://doi.org/10.4049/jimmunol.177.6.3686

Carmack, C.E., S.A. Shinton, K. Hayakawa, and R.R. Hardy. 1990. Rearrangement and selection of VH11 in the Ly-1 B cell lineage. *J. Exp. Med.* 172:371–374. https://doi.org/10.1084/jem.172.1.371

Chen, Y., Y.-B. Park, E. Patel, and G.J. Silverman. 2009. IgM antibodies to apoptosis-associated determinants recruit C1q and enhance dendritic cell phagocytosis of apoptotic cells. *J. Immunol.* 182:6031–6043. https://doi.org/10.4049/jimmunol.0804191

Choi, Y.S., and N. Baumgarth. 2008. Dual role for B-1a cells in immunity to influenza virus infection. *J. Exp. Med.* 205:3053–3064. https://doi.org/10.1084/jem.20080979

Choi, Y.S., J.A. Dieter, K. Rothaeusler, Z. Luo, and N. Baumgarth. 2012. B-1 cells in the bone marrow are a significant source of natural IgM. *Eur. J. Immunol.* 42:120–129. https://doi.org/10.1002/eji.201141890

Conger, J.D., H.J. Sage, S. Kawaguchi, and R.B. Corley. 1991. Properties of murine antibodies from different V region families specific for bromelain-treated mouse erythrocytes. *J. Immunol.* 146:1216–1219. https://doi.org/10.4049/jimmunol.146.4.1216

Doucett, V.P., W. Gerhard, K. Owler, D. Curry, L. Brown, and N. Baumgarth. 2005. Enumeration and characterization of virus-specific B cells by multicolor flow cytometry. *J. Immunol. Methods*. 303:40–52. https://doi.org/10.1016/j.jim.2005.05.014

Ehrenstein, M.R., H.T. Cook, and M.S. Neuberger. 2000. Deficiency in serum immunoglobulin (Ig)M predisposes to development of IgG autoantibodies. *J. Exp. Med.* 191:1253–1258. https://doi.org/10.1084/jem.191.7.1253

Ehrenstein, M.R., and C.A. Notley. 2010. The importance of natural IgM: Scavenger, protector and regulator. *Nat. Rev. Immunol.* 10:778–786. https://doi.org/10.1038/nri2849

Ekiert, D.C., A.K. Kashyap, J. Steel, A. Rubrum, G. Bhabha, R. Khayat, J.H. Lee, M.A. Dillon, R.E. O'Neil, A.M. Faynboym, et al. 2012. Cross-neutralization of influenza A viruses mediated by a single antibody loop. *Nature*. 489:526–532. https://doi.org/10.1038/nature11414

Feeney, A.J. 1990. Lack of N regions in fetal and neonatal mouse immunoglobulin V-D-J junctional sequences. *J. Exp. Med.* 172:1377–1390. https://doi.org/10.1084/jem.172.5.1377

Förster, I., and K. Rajewsky. 1987. Expansion and functional activity of Ly-1$^+$ B cells upon transfer of peritoneal cells into allotype-congenic, newborn mice. *Eur. J. Immunol.* 17:521–528. https://doi.org/10.1002/eji.1830170414

Gershon, R.K. 1974. T cell control of antibody production. *Contemp. Top. Immunobiol.* 3:1–40. https://doi.org/10.1007/978-1-4684-3045-5_1

Glatman Zaretsky, A., C. Konradt, F. Dépis, J.B. Wing, R. Goenka, D.G. Atria, J.S. Silver, S. Cho, A.I. Wolf, W.J. Quinn, et al. 2017. T regulatory cells support plasma cell populations in the bone marrow. *Cell Rep.* 18:1906–1916. https://doi.org/10.1016/j.celrep.2017.01.067

Goldstein, M.F., A.L. Goldstein, E.H. Dunsky, D.J. Dvorin, G.A. Belecanech, and K. Shamir. 2006. Selective IgM immunodeficiency: Retrospective analysis of 36 adult patients with review of the literature. *Ann. Allergy Asthma Immunol.* 97:717–730. https://doi.org/10.1016/S1081-1206(10)60962-3

Goodridge, A., T. Zhang, T. Miyata, S. Lu, and L.W. Riley. 2014. Antiphospholipid IgM antibody response in acute and chronic *Mycobacterium tuberculosis* mouse infection model. *Clin. Respir. J.* 8:137–144. https://doi.org/10.1111/crj.12049

Griffin, D.O., N.E. Holodick, and T.L. Rothstein. 2011. Human B1 cells in umbilical cord and adult peripheral blood express the novel phenotype CD20$^+$ CD27$^+$ CD43$^+$ CD70$^-$. *J. Exp. Med.* 208:67–80. https://doi.org/10.1084/jem.20101499

Gu, Z., L. Gu, R. Eils, M. Schlesner, and B. Brors. 2014. Circlize implements and enhances circular visualization in R. *Bioinformatics*. 30:2811–2812. https://doi.org/10.1093/bioinformatics/btu393

Guo, C., Q. Wang, X. Cao, Y. Yang, X. Liu, L. An, R. Cai, M. Du, G. Wang, Y. Qiu, et al. 2016. High-Throughput sequencing reveals immunological characteristics of the TRB-/IgH-CDR3 region of umbilical cord blood. *J. Pediatr.* 176:69–78.e1. https://doi.org/10.1016/j.jpeds.2016.05.078

Gupta, S., and A. Gupta. 2017. Selective IgM deficiency-an underestimated primary immunodeficiency. *Front. Immunol.* 8:1056. https://doi.org/10.3389/fimmu.2017.01056

Haas, K.M., J.C. Poe, D.A. Steeber, and T.F. Tedder. 2005. B-1a and B-1b cells exhibit distinct developmental requirements and have unique functional roles in innate and adaptive immunity to *S. pneumoniae*. *Immunity*. 23:7–18. https://doi.org/10.1016/j.immuni.2005.04.011

Hardy, R.R., C.E. Carmack, S.A. Shinton, R.J. Riblet, and K. Hayakawa. 1989. A single VH gene is utilized predominantly in anti-BrMRBC hybridomas derived from purified Ly-1 B cells. Definition of the VH11 family. *J. Immunol.* 142:3643–3651. https://doi.org/10.4049/jimmunol.142.10.3643

Haury, M., A. Sundblad, A. Grandien, C. Barreau, A. Coutinho, and A. Nobrega. 1997. The repertoire of serum IgM in normal mice is largely independent of external antigenic contact. *Eur. J. Immunol.* 27:1557–1563. https://doi.org/10.1002/eji.1830270635

Hayakawa, K., M. Asano, S.A. Shinton, M. Gui, D. Allman, C.L. Stewart, J. Silver, and R.R. Hardy. 1999. Positive selection of natural autoreactive B cells. *Science*. 285:113–116. https://doi.org/10.1126/science.285.5424.113

Hayakawa, K., M. Asano, S.A. Shinton, M. Gui, L.J. Wen, J. Dashoff, and R.R. Hardy. 2003. Positive selection of anti-thy-1 autoreactive B-1 cells and natural serum autoantibody production independent from bone marrow B cell development. *J. Exp. Med.* 197:87–99. https://doi.org/10.1084/jem.20021459

Hayakawa, K., C.E. Carmack, S.A. Shinton, and R.R. Hardy. 1992. Selection of autoantibody specificities in the Ly-1 B subset. *Ann. N. Y. Acad. Sci.* 651:346–353. https://doi.org/10.1111/j.1749-6632.1992.tb24634.x

Hayakawa, K., and R.R. Hardy. 2000. Development and function of B-1 cells. *Curr. Opin. Immunol.* 12:346–353. https://doi.org/10.1016/S0952-7915(00)00098-4

Hayakawa, K., R.R. Hardy, M. Honda, L.A. Herzenberg, A.D. Steinberg, and L.A. Herzenberg. 1984. Ly-1 B cells: Functionally distinct lymphocytes that secrete IgM autoantibodies. *Proc. Natl. Acad. Sci. USA*. 81:2494–2498. https://doi.org/10.1073/pnas.81.8.2494

Heyman, B. 2000. Regulation of antibody responses via antibodies, complement, and Fc receptors. *Annu. Rev. Immunol.* 18:709–737. https://doi.org/10.1146/annurev.immunol.18.1.709

Holodick, N.E., and T.L. Rothstein. 2015. B cells in the aging immune system: Time to consider B-1 cells. *Ann. N. Y. Acad. Sci.* 1362:176–187. https://doi.org/10.1111/nyas.12825

Holodick, N.E., T. Vizconde, T.J. Hopkins, and T.L. Rothstein. 2016. Age-related decline in natural IgM function: Diversification and selection of the B-1a cell pool with age. *J. Immunol.* 196:4348–4357. https://doi.org/10.4049/jimmunol.1600073

Hooijkaas, H., A.A. van der Linde-Preesman, S. Benne, and R. Benner. 1985. Frequency analysis of the antibody specificity repertoire of mitogen-reactive B cells and "spontaneously" occurring "background" plaque-forming cells in nude mice. *Cell. Immunol.* 92:154–162. https://doi.org/10.1016/0008-8749(85)90073-5

Hsu, L.-H., K.-P. Li, K.-H. Chu, and B.-L. Chiang. 2014. A B-1a cell subset induces Foxp3– T cells with regulatory activity through an IL-10-independent pathway. *Cell Mol. Immunol.* 12:354–365. https://doi.org/10.1038/cmi.2014.56

Ichikawa, D., M. Asano, S.A. Shinton, J. Brill-Dashoff, A.M. Formica, A. Velcich, R.R. Hardy, and K. Hayakawa. 2015. Natural anti-intestinal goblet cell autoantibody production from marginal zone B cells. *J. Immunol.* 194:606–614. https://doi.org/10.4049/jimmunol.1402383

Ise, W., and T. Kurosaki. 2021. Plasma cell generation during T-cell-dependent immune responses. *Int. Immunol.* 33:797–801. https://doi.org/10.1093/intimm/dxab071

Jackson-Jones, L.H., S.M. Duncan, M.S. Magalhaes, S.M. Campbell, R.M. Maizels, H.J. McSorley, J.E. Allen, and C. Bénézech. 2016. Fat-associated lymphoid clusters control local IgM secretion during pleural infection and lung inflammation. *Nat. Commun.* 7:1–14. https://doi.org/10.1038/ncomms12651

Jayasekera, J.P., E.A. Moseman, and M.C. Carroll. 2007. Natural antibody and complement mediate neutralization of influenza virus in the absence of

prior immunity. *J. Virol.* 81:3487–3494. https://doi.org/10.1128/jvi.02128-06

Kantor, A.B., and L.A. Herzenberg. 1993. Origin of murine B cell lineages. *Annu. Rev. Immunol.* 11:501–538. https://doi.org/10.1146/annurev.iy.11.040193.002441

Kawahara, T., H. Ohdan, G. Zhao, Y.G. Yang, and M. Sykes. 2003. Peritoneal cavity B cells are precursors of splenic IgM natural antibody-producing cells. *J. Immunol.* 171:5406–5414. https://doi.org/10.4049/jimmunol.171.10.5406

Kearney, J.F., P. Patel, E.K. Stefanov, and R.G. King. 2015. Natural antibody repertoires: Development and functional role in inhibiting allergic airway disease. *Annu. Rev. Immunol.* 33:475–504. https://doi.org/10.1146/annurev-immunol-032713-120140

Keightley, R.G., M.D. Cooper, and A.R. Lawton. 1976. The T cell dependence of B cell differentiation induced by pokeweed mitogen. *J. Immunol.* 117:1538–1544. https://doi.org/10.4049/jimmunol.117.5_Part_1.1538

Kenny, J.J., L.J. Yaffe, A. Ahmed, and E.S. Metcalf. 1983. Contribution of Lyb 5^+ and Lyb 5^- B cells to the primary and secondary phosphocholine-specific antibody response. *J. Immunol.* 130:2574–2579. https://doi.org/10.4049/jimmunol.130.6.2574

Kopf, M., F. Brombacher, P.D. Hodgkin, A.J. Ramsay, E.A. Milbourne, W.J. Dai, K.S. Ovington, C.A. Behm, G. Köhler, I.G. Young, and K.I. Matthaei. 1996. IL-5-deficient mice have a developmental defect in $CD5^+$ B-1 cells and lack eosinophilia but have normal antibody and cytotoxic T cell responses. *Immunity.* 4:15–24. https://doi.org/10.1016/S1074-7613(00)80294-0

Kreuk, L.S.M., M.A. Koch, L.C. Slayden, N.A. Lind, S. Chu, H.P. Savage, A.B. Kantor, N. Baumgarth, and G.M. Barton. 2019. B cell receptor and Toll-like receptor signaling coordinate to control distinct B-1 responses to both self and the microbiota. *Elife.* 8:e47015. https://doi.org/10.7554/eLife.47015

Lalor, P.A., L.A. Herzenberg, S. Adams, and A.M. Stall. 1989. Feedback regulation of murine Ly-1 B cell development. *Eur. J. Immunol.* 19:507–513. https://doi.org/10.1002/eji.1830190315

Li, Y.S., Y. Zhou, L. Tang, S.A. Shinton, K. Hayakawa, and R.R. Hardy. 2015. A developmental switch between fetal and adult B lymphopoiesis. *Ann. N. Y. Acad. Sci.* 1362:8–15. https://doi.org/10.1111/nyas.12769

Madsen, L., N. Labrecque, J. Engberg, A. Dierich, A. Svejgaard, C. Benoist, D. Mathis, and L. Fugger. 1999. Mice lacking all conventional MHC class II genes. *Proc. Natl. Acad. Sci. USA.* 96:10338–10343. https://doi.org/10.1073/pnas.96.18.10338

Margry, B., W.H. Wieland, P.J. van Kooten, W. van Eden, and F. Broere. 2013. Peritoneal cavity B-1a cells promote peripheral $CD4^+$ T-cell activation. *Eur. J. Immunol.* 43:2317–2326. https://doi.org/10.1002/eji.201343418

McKay, J.T., M.A. Haro, C.A. Daly, R.D. Yammani, B. Pang, W.E. Swords, and K.M. Haas. 2017. PD-L2 regulates B-1 cell antibody production against phosphorylcholine through an IL-5-dependent mechanism. *J. Immunol.* 199:2020–2029. https://doi.org/10.4049/jimmunol.1700555

Mercolino, T.J., L.W. Arnold, L.A. Hawkins, and G. Haughton. 1988. Normal mouse peritoneum contains a large population of $Ly\text{-}1^+$ (CD5) B cells that recognize phosphatidyl choline. Relationship to cells that secrete hemolytic antibody specific for autologous erythrocytes. *J. Exp. Med.* 168:687–698. https://doi.org/10.1084/jem.168.2.687

Mi, Q.S., L. Zhou, D.H. Schulze, R.T. Fischer, A. Lustig, L.J. Rezanka, D.M. Donovan, D.L. Longo, and J.J. Kenny. 2000. Highly reduced protection against *Streptococcus pneumoniae* after deletion of a single heavy chain gene in mouse. *Proc. Natl. Acad. Sci. USA.* 97:6031–6036. https://doi.org/10.1073/pnas.110039497

Mombaerts, P., A.R. Clarke, M.A. Rudnicki, J. Iacomini, S. Itohara, J.J. Lafaille, L. Wang, Y. Ichikawa, R. Jaenisch, M.L. Hooper, and S. Tonegawa. 1992. Mutations in T-cell antigen receptor genes α and β block thymocyte development at different stages. *Nature.* 360:225–231. https://doi.org/10.1038/360225a0

Montecino-Rodriguez, E., and K. Dorshkind. 2012. B-1 B cell development in the fetus and adult. *Immunity.* 36:13–21. https://doi.org/10.1016/j.immuni.2011.11.017

Moon, B.G., S. Takaki, K. Miyake, and K. Takatsu. 2004. The role of IL-5 for mature B-1 cells in homeostatic proliferation, cell survival, and Ig production. *J. Immunol.* 172:6020–6029. https://doi.org/10.4049/jimmunol.172.10.6020

New, J.S., B.L.P. Dizon, C.F. Fucile, A.F. Rosenberg, J.F. Kearney, and R.G. King. 2020. Neonatal exposure to commensal-bacteria-derived antigens directs polysaccharide-specific B-1 B cell repertoire development. *Immunity.* 53:172–186.e6. https://doi.org/10.1016/j.immuni.2020.06.006

Nguyen, T.T.T., R.A. Elsner, and N. Baumgarth. 2015. Natural IgM prevents autoimmunity by enforcing B cell central tolerance induction. *J. Immunol.* 194:1489–1502. https://doi.org/10.4049/jimmunol.1401880

Nguyen, T.T.T., B.A. Graf, T.D. Randall, and N. Baumgarth. 2017. sIgM-FcμR interactions regulate early B cell activation and plasma cell development after influenza virus infection. *J. Immunol.* 199:1635–1646. https://doi.org/10.4049/jimmunol.1700560

Noelle, R.J., J.A. Ledbetter, and A. Aruffo. 1992. CD40 and its ligand, an essential ligand-receptor pair for thymus-dependent B-cell activation. *Immunol. Today.* 13:431–433. https://doi.org/10.1016/0167-5699(92)90068-I

Notley, C.A., M.A. Brown, G.P. Wright, and M.R. Ehrenstein. 2011. Natural IgM is required for suppression of inflammatory arthritis by apoptotic cells. *J. Immunol.* 186:4967–4972. https://doi.org/10.4049/jimmunol.1003021

Ochsenbein, A.F., T. Fehr, C. Lutz, M. Suter, F. Brombacher, H. Hengartner, and R.M. Zinkernagel. 1999. Control of early viral and bacterial distribution and disease by natural antibodies. *Science.* 286:2156–2159. https://doi.org/10.1126/science.286.5447.2156

Ogden, C.A., R. Kowalewski, Y. Peng, V. Montenegro, and K.B. Elkon. 2009. IGM is required for efficient complement mediated phagocytosis of apoptotic cells in vivo. *Autoimmunity.* 38:259–264. https://doi.org/10.1080/08916930500124452

Van Oudenaren, A., J.J. Haaijman, and R. Benner. 1984. Frequencies of background cytoplasmic Ig-containing cells in various lymphoid organs of athymic and euthymic mice as a function of age and immune status. *Immunology.* 51:735–742

Patel, P.S., and J.F. Kearney. 2015. Neonatal exposure to pneumococcal phosphorylcholine modulates the development of house dust mite allergy during adult life. *J. Immunol.* 194:5838–5850. https://doi.org/10.4049/jimmunol.1500251

Prohaska, T.A., X. Que, C.J. Diehl, S. Hendrikx, M.W. Chang, K. Jepsen, C.K. Glass, C. Benner, and J.L. Witztum. 2018. Massively parallel sequencing of peritoneal and splenic B cell repertoires highlights unique properties of B-1 cell antibodies. *J. Immunol.* 200:1702–1717. https://doi.org/10.4049/jimmunol.1700568

Quartier, P., P.K. Potter, M.R. Ehrenstein, M.J. Walport, and M. Botto. 2005. Predominant role of IgM-dependent activation of the classical pathway in the clearance of dying cells by murine bone marrow-derived macrophages in vitro. *Eur. J. Immunol.* 35:252–260. https://doi.org/10.1002/eji.200425497

Que, X., M.Y. Hung, C. Yeang, A. Gonen, T.A. Prohaska, X. Sun, C. Diehl, A. Määttä, D.E. Gaddis, K. Bowden, et al. 2018. Oxidized phospholipids are proinflammatory and proatherogenic in hypercholesterolaemic mice. *Nature.* 558:301–306. https://doi.org/10.1038/s41586-018-0198-8

R Core Team. 2020. R: A language and environment for statistical computing. *R Foundation for Statistical Computing, Vienna, Austria.* https://www.R-project.org/.

Rettig, T.A., C. Ward, B.A. Bye, M.J. Pecaut, and S.K. Chapes. 2018. Characterization of the naive murine antibody repertoire using unamplified high-throughput sequencing. *PLoS One.* 13:e0190982. https://doi.org/10.1371/journal.pone.0190982

Reynolds, A.E., M. Kuraoka, and G. Kelsoe. 2015. Natural IgM is produced by CD5- plasma cells that occupy a distinct survival niche in bone marrow. *J. Immunol.* 194:231–242. https://doi.org/10.4049/jimmunol.1401203

Rothaeusler, K., and N. Baumgarth. 2006. Evaluation of intranuclear BrdU detection procedures for use in multicolor flow cytometry. *Cytometry A.* 69:249–259. https://doi.org/10.1002/cyto.a.20252

Savage, H.P., K. Kläsener, F.L. Smith, Z. Luo, M. Reth, and N. Baumgarth. 2019. TLR induces reorganization of the IgM-BCR complex regulating murine B-1 cell responses to infections. *Elife.* 8:e46997. https://doi.org/10.7554/eLife.46997

Savage, H.P., V.M. Yenson, S.S. Sawhney, B.J. Mousseau, F.E. Lund, and N. Baumgarth. 2017. Blimp-1-dependent and -independent natural antibody production by B-1 and B-1-derived plasma cells. *J. Exp. Med.* 214:2777–2794. https://doi.org/10.1084/jem.20161122

Savitsky, D., and K. Calame. 2006. B-1 B lymphocytes require Blimp-1 for immunoglobulin secretion. *J. Exp. Med.* 203:2305–2314. https://doi.org/10.1084/jem.20060411

Shapiro-Shelef, M., K.I. Lin, L.J. McHeyzer-Williams, J. Liao, M.G. McHeyzer-Williams, and K. Calame. 2003. Blimp-1 is required for the formation of immunoglobulin secreting plasma cells and pre-plasma memory B cells. *Immunity.* 19:607–620. https://doi.org/10.1016/S1074-7613(03)00267-X

Smith, F.L., and N. Baumgarth. 2019. B-1 cell responses to infections. *Curr. Opin. Immunol.* 57:23–31. https://doi.org/10.1016/j.coi.2018.12.001

Stall, A.M., S. Adams, L.A. Herzenberg, and A.B. Kantor. 1992. Characteristics and development of the murine B-1b (Ly-1 B sister) cell population. *Ann. N. Y. Acad. Sci.* 651:33–43. https://doi.org/10.1111/j.1749-6632.1992.tb24591.x

Suo, C., E. Dann, I. Goh, L. Jardine, V. Kleshchevnikov, J.E. Park, R.A. Botting, E. Stephenson, J. Engelbert, Z.K. Tuong, et al. 2022. Mapping the developing human immune system across organs. *Science*. 376:eabo0510. https://doi.org/10.1126/science.abo0510

Takeuchi, T., T. Nakagawa, Y. Maeda, S. Hirano, M. Sasaki-Hayashi, S. Makino, A. Shimizu, T. Takeuchi, T. Nakagawa, Y. Maeda, et al. 2009. Functional defect of B lymphocytes in a patient with selective IgM deficiency associated with systemic lupus erythematosus. *Autoimmunity*. 34:115–122. https://doi.org/10.3109/08916930109001959

Tipton, C.M., C.F. Fucile, J. Darce, A. Chida, T. Ichikawa, I. Gregoretti, S. Schieferl, J. Hom, S. Jenks, R.J. Feldman, et al. 2015. Diversity, cellular origin and autoreactivity of antibody-secreting cell population expansions in acute systemic lupus erythematosus. *Nat. Immunol.* 16:755–765. https://doi.org/10.1038/ni.3175

Upadhye, A., P. Srikakulapu, A. Gonen, S. Hendrikx, H.M. Perry, A. Nguyen, C. McSkimming, M.A. Marshall, J.C. Garmey, A.M. Taylor, et al. 2019. Diversification and CXCR4-dependent establishment of the bone marrow B-1a cell pool governs atheroprotective IgM production linked to human coronary atherosclerosis. *Circ. Res.* 125:e55–e70. https://doi.org/10.1161/CIRCRESAHA.119.315786

Waffarn, E.E., C.J. Hastey, N. Dixit, Y. Soo Choi, S. Cherry, U. Kalinke, S.I. Simon, and N. Baumgarth. 2015. Infection-induced type I interferons activate CD11b on B-1 cells for subsequent lymph node accumulation. *Nat. Commun.* 6:8991. https://doi.org/10.1038/ncomms9991

Wagih, O. 2017. ggseqlogo: A 'ggplot2' Extension for Drawing Publication-Ready Sequence Logos. *R package version 0.1*. https://CRAN.R-project.org/package=ggseqlogo.

Wang, H., D.M. Shin, S. Abbasi, S. Jain, A.L. Kovalchuk, N. Beaty, S. Chen, I. Gonzalez-Garcia, and H.C. Morse III. 2012. Expression of plasma cell alloantigen 1 defines layered development of B-1a B-cell subsets with distinct innate-like functions. *Proc. Natl. Acad. Sci. USA*. 109:20077–20082. https://doi.org/10.1073/pnas.1212428109

Wang, X., K. Ma, M. Chen, K.-H. Ko, B.-J. Zheng, and L. Lu. 2016. IL-17A promotes pulmonary B-1a cell differentiation via induction of blimp-1 expression during influenza virus infection. *PLoS Pathog*. 12:e1005367. https://doi.org/10.1371/journal.ppat.1005367

Wardemann, H., T. Boehm, N. Dear, and R. Carsetti. 2002. B-1a B cells that link the innate and adaptive immune responses are lacking in the absence of the spleen. *J. Exp. Med.* 195:771–780. https://doi.org/10.1084/jem.20011140

Wasserman, R., Y.S. Li, S.A. Shinton, C.E. Carmack, T. Manser, D.L. Wiest, K. Hayakawa, and R.R. Hardy. 1998. A novel mechanism for B cell repertoire maturation based on response by B cell precursors to pre-B receptor assembly. *J. Exp. Med.* 187:259–264. https://doi.org/10.1084/jem.187.2.259

Wong, J.B., S.L. Hewitt, L.M. Heltemes-Harris, M. Mandal, K. Johnson, K. Rajewsky, S.B. Koralov, M.R. Clark, M.A. Farrar, and J.A. Skok. 2019. B-1a cells acquire their unique characteristics by bypassing the pre-BCR selection stage. *Nat. Commun.* 10:4768. https://doi.org/10.1038/s41467-019-12824-z

Yang, Y., C. Wang, Q. Yang, A.B. Kantor, H. Chu, E.E.B. Ghosn, G. Qin, S.K. Mazmanian, J. Han, and L.A. Herzenberg. 2015. Distinct mechanisms define murine B cell lineage immunoglobulin heavy chain (IgH) repertoires. *Elife*. 4:e09083. https://doi.org/10.7554/eLife.09083

Yu, L., and Y. Guan. 2014. Immunologic basis for long HCDR3s in broadly neutralizing antibodies against HIV-1. *Front. Immunol.* 5:250. https://doi.org/10.3389/fimmu.2014.00250

Yuan, J., C.K. Nguyen, X. Liu, C. Kanellopoulou, and S.A. Muljo. 2012. Lin28b reprograms adult bone marrow hematopoietic progenitors to mediate fetal-like lymphopoiesis. *Science*. 335:1195–1200. https://doi.org/10.1126/science.1216557

Zeng, Z., B.G.J. Surewaard, C.H.Y. Wong, C. Guettler, B. Petri, R. Burkhard, M. Wyss, H. Le Moual, R. Devinney, G.C. Thompson, et al. 2018. Sex-hormone-driven innate antibodies protect females and infants against EPEC infection. *Nat. Immunol.* 19:1100–1111. https://doi.org/10.1038/s41590-018-0211-2

Zimecki, M., and J.A. Kapp. 1994. Presentation of antigen by B cell subsets. II. The role of CD5 B cells in the presentation of antigen to antigen-specific T cells. *Arch. Immunol. Ther. Exp.* 42:349–353

Zimecki, M., P.J. Whiteley, C.W. Pierce, and J.A. Kapp. 1994. Presentation of antigen by B cells subsets. I. Lyb-5$^+$ and Lyb-5$^-$ B cells differ in ability to stimulate antigen specific T cells. *Arch. Immunol. Ther. Exp.* 42:115–123

JEM

Supplemental material

Figure S1. **BM B-1PC do not contribute autoreactive IgM to the nIgM repertoire.** Heatmap indicating the binding intensity of serum IgM against an array of indicated auto-antigens. Sera were taken from female T cell–deficient TCR $\beta/\delta^{-/-}$ mice (n = 6), control C57BL/6 (n = 6) mice, B cell Ig-allotype chimera CD4-depleted via treatment with anti-CD4 mAb (n = 4), B cell Ig-allotype chimera CD4, T cell sufficient (n = 4), $Rag1^{-/-}$ mice reconstituted with B-1 cells only (n = 5), and $Rag1^{-/-}$ mice reconstituted with B-1 cells and $CD4^+$ T cells (n = 5).

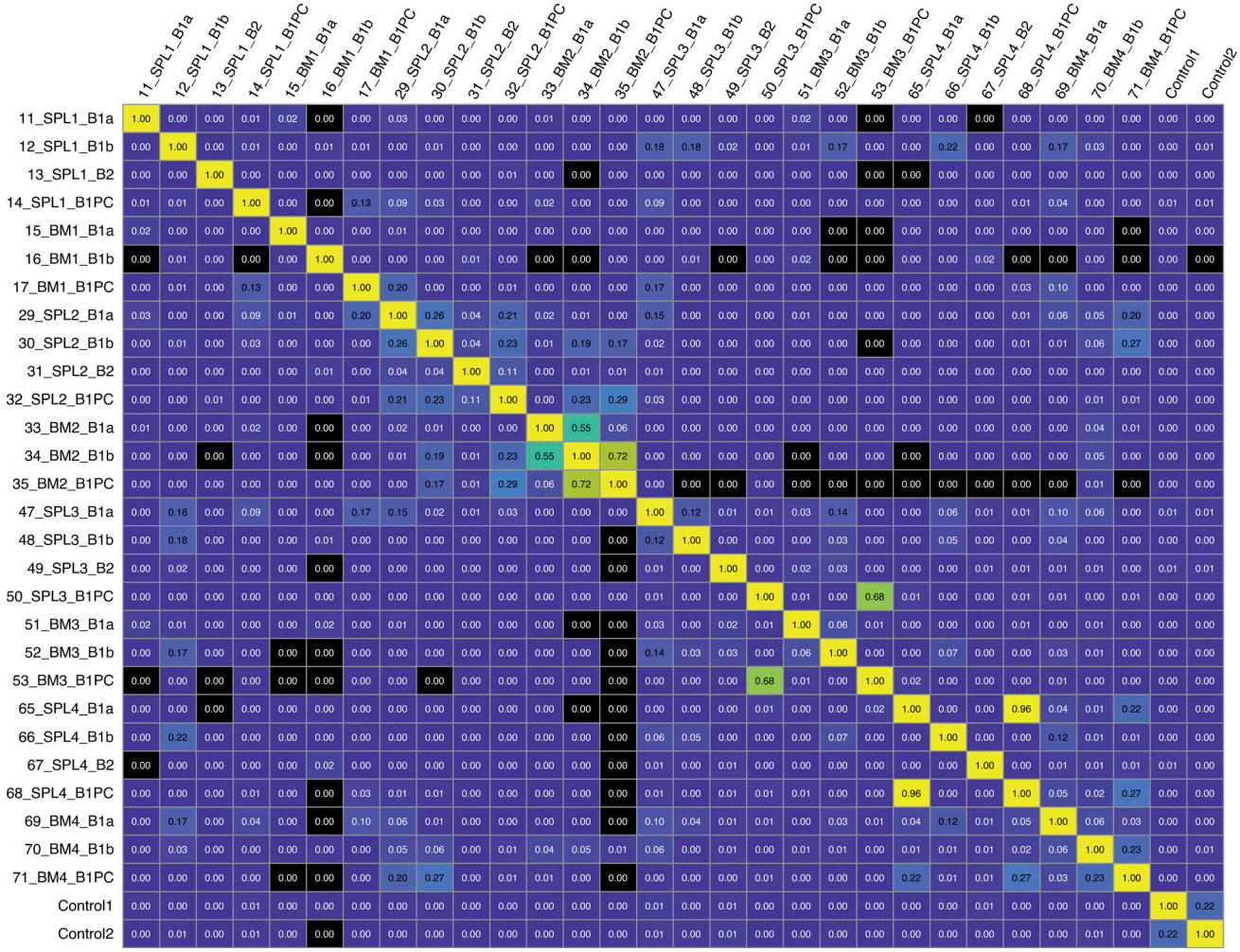

Figure S2. **B-1PC from spleen and BM in the same mouse consistently have overlapping repertoire.** Morisita overlap index plot showing relatedness of Igh-chain sequences obtained by bulk RNA BCR sequencing from FACS-purified populations of live, non-dump, CD19^{hi} CD43^{+} IgM^{+} CD5^{+} B-1a; live, non-dump, CD19^{hi} CD43^{+} IgM^{+} CD5^{-} B-1b; live, non-dump CD23^{-} IgM^{+} Blimp-1^{+} B-1PC from spleen and BM and live, non-dump, CD19^{+} CD23^{+} follicular B cells (B-2) from spleen of four individual Blimp-1YFP reporter mice. Controls were mixed spleen cells from two C57BL/6 mice.

Provided online are Table S1, Table S2, and Table S3. Table S1 shows N-region insertions in the most common clones identified in B-1PC. Table S2 lists antibodies and fluorescent reagents used for ELISA, ELISPOT, and flow cytometry. Table S3 lists PCR primers used for BCR sequencing of B-1 cell populations.